



HAL
open science

Design, Synthesis, and Biological Evaluation of New Type of Gemini Analogues with a Cyclopropane Moiety in Their Side Chain

Uxía Gómez-Bouzó, Carole Peluso-Iltis, Hugo Santalla, Mario Alfredo Quevedo, Lieve Verlinden, Annemieke Verstuyf, Yagamare Fall, Generosa Gómez, Natacha Rochel

► To cite this version:

Uxía Gómez-Bouzó, Carole Peluso-Iltis, Hugo Santalla, Mario Alfredo Quevedo, Lieve Verlinden, et al.. Design, Synthesis, and Biological Evaluation of New Type of Gemini Analogues with a Cyclopropane Moiety in Their Side Chain. *Journal of Medicinal Chemistry*, 2024, 67 (12), pp.10386-10400. 10.1021/acs.jmedchem.4c00854 . hal-04687990

HAL Id: hal-04687990

<https://hal.science/hal-04687990v1>

Submitted on 4 Sep 2024

HAL is a multi-disciplinary open access archive for the deposit and dissemination of scientific research documents, whether they are published or not. The documents may come from teaching and research institutions in France or abroad, or from public or private research centers.

L'archive ouverte pluridisciplinaire **HAL**, est destinée au dépôt et à la diffusion de documents scientifiques de niveau recherche, publiés ou non, émanant des établissements d'enseignement et de recherche français ou étrangers, des laboratoires publics ou privés.

Design, Synthesis and Biological Evaluation of a new type of Gemini Analogues With a Cyclopropane moiety in Their Side Chain.

Uxía Gómez-Bouzó,¹ Carole Peluso-Iltis,^{2,3,4,5} Hugo Santalla,¹ Mario Alfredo Quevedo,^{6*} Lieve Verlinden,⁷ Annemieke Verstuyf,⁷ Yagamare Fall,^{1*} Generosa Gómez¹ and Natacha Rochel^{2,3,4,5*}

¹Departamento de Química Orgánica and Instituto de Investigación Sanitaria Galicia Sur (IISGS), Campus Lagoas Marcosende, Universidad de Vigo, 36310 Vigo, Spain.

²Institute of Genetics and Molecular and Cellular Biology (IGBMC), Illkirch, 67400, France.

³ CNRS UMR 7104, Illkirch, 67400, France.

⁴ Inserm U1258, Illkirch, 67400, France.

⁵ University of Strasbourg, Illkirch, 67400, France.

⁶Unidad de Investigación y desarrollo en Tecnología Farmacéutica (UNITEFA), CONICET and Departamento de Ciencias Farmacéuticas, Facultad de Ciencias Químicas, Universidad Nacional de Córdoba. X5000HUA, Córdoba, Argentina.

⁷Clinical and Experimental Endocrinology, Department of Chronic Diseases and Metabolism, KU Leuven, 3000 Leuven, Belgium.

*To whom correspondence should be addressed:

(YF) +34 986812323, e-mail: yagamare@uvigo.es

(MAQ) +54 351 5353850 int 55437, e-mail: alfredoq@fcq.unc.edu.ar

(NR) +33.369.48.52.93, e-mail: rochel@igbmc.fr

Key words: Calcitriol, antiproliferative agents, hypercalcemia, cancer, Gemini

Abstract

We synthesized two new gemini analogues **UG-480** and **UG-481** that incorporate a modified longer side chain containing a cyclopropane group. The evaluation of the bioactivities of the two gemini analogues indicated that the 17,20 threo (2*S*) compound, **UG-480**, is the most active one and as active as 1,25(OH)₂D₃. Docking and MD data showed that the compounds bind efficiently to VDR with **UG-480** forming an energetically more favorable interaction with His397. Structural analysis indicated that whereas the **UG-480** compound efficiently stabilizes the active VDR conformation, it induces conformational changes in H6-H7 VDR region that are greater than those induced by the parental Gemini and that this is due to the occupancy of the secondary channel by its modified side chain.

INTRODUCTION

$1\alpha,25$ -dihydroxyvitamin D_3 ($1,25(OH)_2D_3$; calcitriol) (**Figure 1A**), the hormonally active form of vitamin D_3 , has been shown to exhibit a wide variety of antitumor activities, but its therapeutic use is limited due to its severe calcemic side effects at the effective dose required for antitumor activity.¹ Accordingly, there is much interest in the design and synthesis of new calcitriol analogues displaying less toxicity.² The pharmacodynamic interactions pattern between VDR and calcitriol and its analogues has been extensively studied,³⁻⁷ with key pharmacophoric contacts involved in VDR mediated bioactivity. Of note, the bioactive compounds are anchored to VDR through three hydroxyl groups forming hydrogen bonds with three pairs of polar amino acids within the ligand binding pocket and that correspond to the three pharmacophoric contacts (**Figure 1B**). For calcitriol, the 1α -OH group interacts with Tyr143 (helix H1) and Ser278 (helix H5), the 3β -OH group contacts Ser237 (helix H3) and Arg274 (helix H5), and the 25-OH group interacts with His305 (loop between helices H6 and H7) and His397 (helix H11).⁸

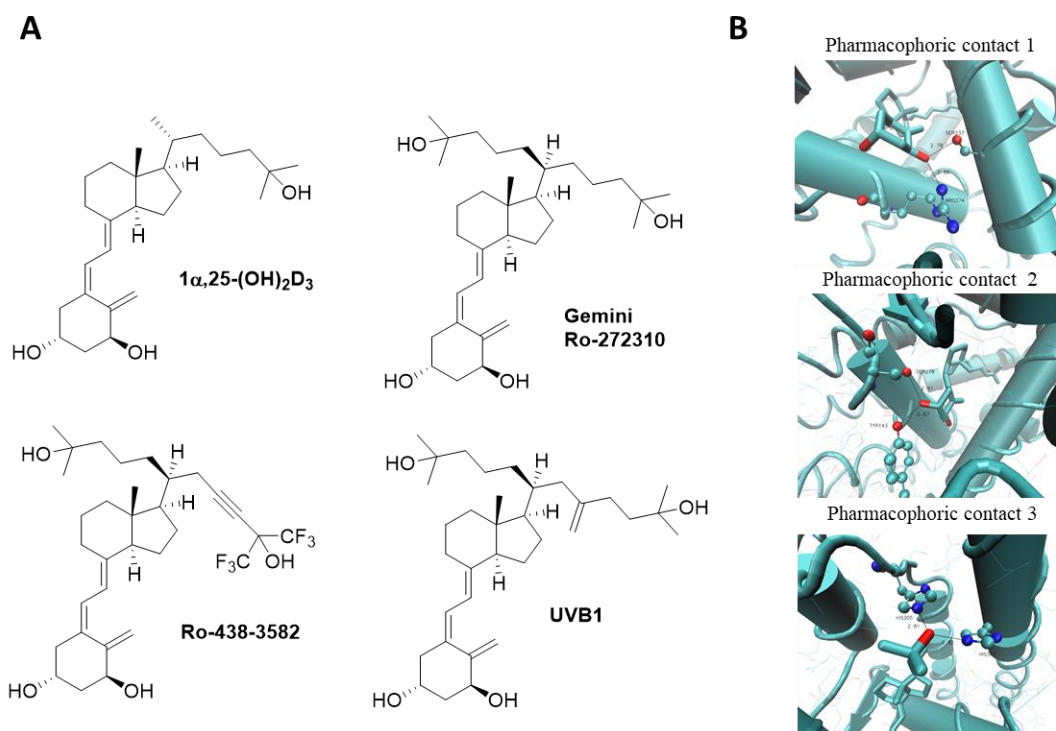


Figure 1. (A) Structures of calcitriol, Gemini and some of its analogues. (B) Pharmacophoric contacts for the binding of calcitriol to VDR.

Among the many new analogues of calcitriol, it's worth mentioning those having a second side chain linked to C-20 and giving rise to a new class of compounds, known as gemini analogues⁹ (**Figure 1A**). The first example of this type of compounds featured a calcitriol analogue with two identical side chains and was coined Gemini (Ro-272310).¹⁰ With the two side chains in Gemini, the possibility of chain modification is increased and the new class of gemini analogues has significantly enlarged the biological spectrum of calcitriol.¹¹ In spite of the obvious interest of pharmaceutical industry and the vitamin D

research groups for the gemini analogues, the current methodologies for the preparation of these analogues lack of flexibility and efficiency in the incorporation of molecular diversity. To the best of our knowledge the only known methodology to access gemini analogues was described by Uskokovic and co-workers.¹² Their procedure relies on an ene reaction for the nonselective generation of the double side chain precursor and the subsequent separation of isomers using expensive techniques for purification and separation of mixtures. Our research group developed a new synthetic procedure for gemini analogues, using a key sigmatropic rearrangement, providing a versatile method to introduce novel side chains to the vitamin D scaffold giving access to a variety of analogues with potentially interesting biological properties. We thus synthesized and patented gemini analogue Ro-438-3582.¹³

During the synthesis of Ro-438-3582, we serendipitously synthesized a new gemini type analogue we coined **UVB1** (**Figure 1**).¹⁴ The *in vivo* biological evaluation showed that it has potent antitumoral effects over a wide range of tumor cell lines and lacks hypercalcemic activity and toxicity effects.¹⁵ Recent research has shown that **UVB1** exhibits antineoplastic activity in breast cancer patient-derived xenograft cells.¹⁶ In view of the excellent biological results of **UVB1**, we hypothesized that the two new gemini analogues with a cyclopropane moiety in their side chain **UG-480** and **UG-481** (**Figure 2**) could be of interest. Incorporation of cyclopropane moiety in the side chain of 1,25(OH)₂D₃ increases its rigidity and enhances its interactions contributing to a more stable VDR agonist conformation.¹⁷

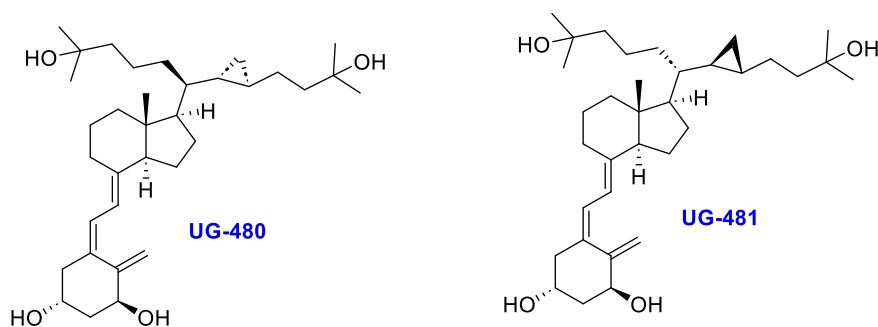
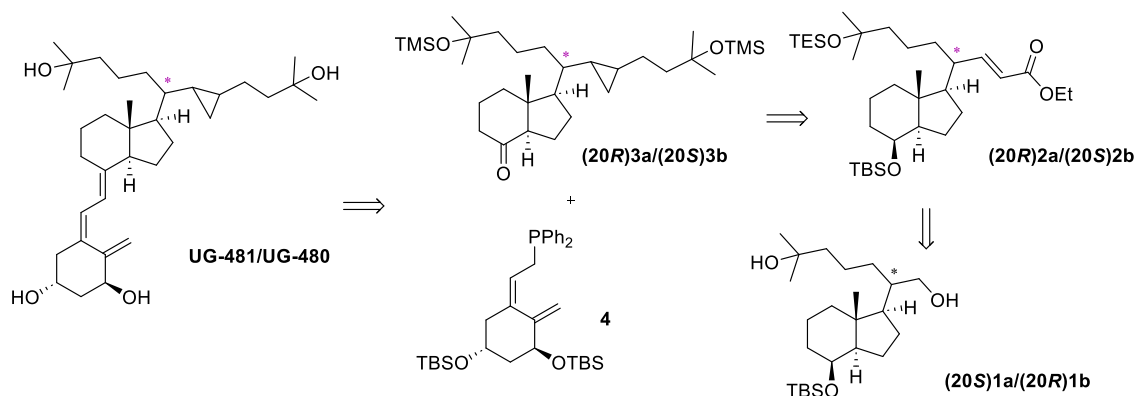


Figure 2. Structures of two new gemini analogues with a cyclopropane moiety in their side chain.

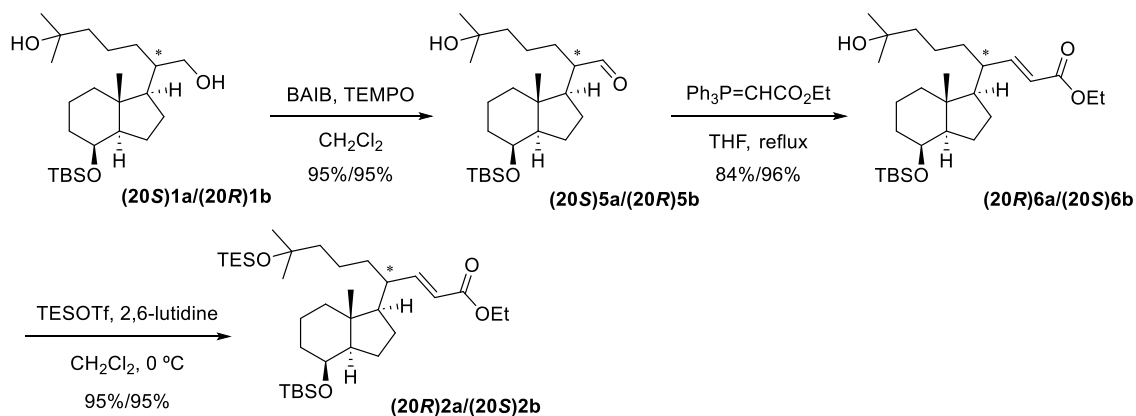
RESULTS AND DISCUSSION

Design. We anticipated that the two gemini-type analogues **UG-480** and **UG-481** could be synthesized from chiral diols (*S*)**1a** and (*R*)**1b** which involves the construction of Grundmann's ketones **3a/3b** followed by Wittig-Horner coupling using phosphine oxide **4** to afford the target compounds. The retrosynthetic analysis for **UG-480** and **UG-481** is depicted in **Scheme 1**.



Scheme 1. Retrosynthetic analysis for gemini type analogues **UG-480** and **UG-481**.

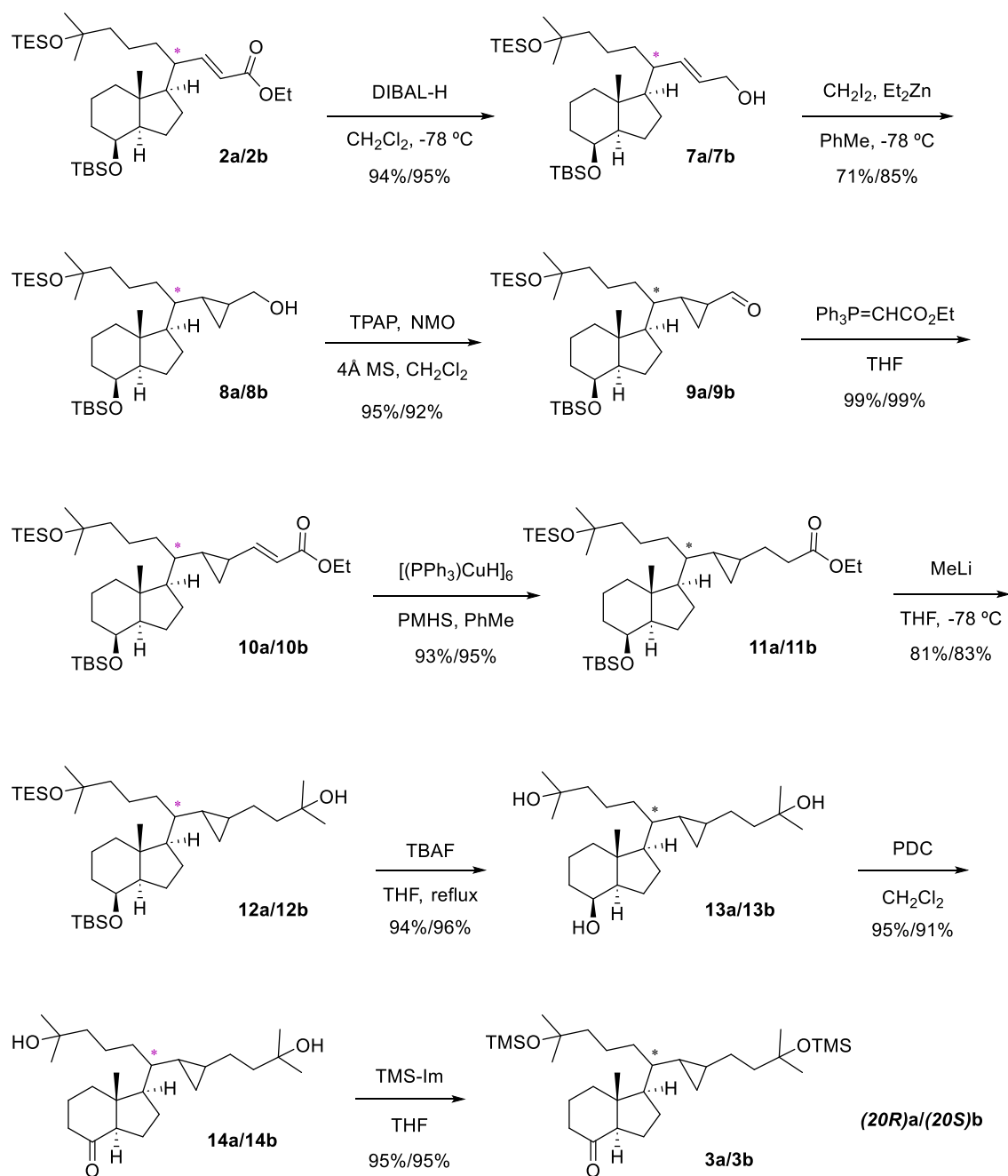
Chemistry. Diols (*S*)**1a** and (*R*)**1b** were synthesized from commercially available Inhoffen Lythgoe diol, using a [3,3]-sigmatropic allylic rearrangement as previously reported.¹⁸ Accordingly, chiral esters **2a/2b** were prepared as outlined in **Scheme 2**.



Scheme 2. Synthesis of esters **2a/2b**

TEMPO oxidation of alcohols **1a/1b**, followed by Wittig reaction of the resulting aldehydes **5a/5b** afforded esters **6a/6b** in 80%/91% overall yield (2 steps). Triethylsilyl protection of the hydroxyl group of **6a/6b** gave 95%/95% yield of the esters **2a/2b**.

Ketones **3a/3b** could be easily prepared from esters **2a/2b** by side chain elaboration as shown in **Scheme 3**.



Scheme 3. Synthesis of Grundmann's ketones **3a/3b**.

DIBAL-H reduction of esters **2a/2b** afforded alcohols **7a/7b** in 94%/95% yield. Simmons-Smith cyclopropanation of allylic alcohols **7a/7b** gave the cyclopropyl compounds **8a/8b** with 83% dr(**8a**)/93% dr(**8b**). The high stereoselectivity of the cyclopropanation can be understood by a chelation mechanism between the Zn²⁺ and the alcohol group in the reaction intermediate as shown in the Newman projections (**Figure 3**).

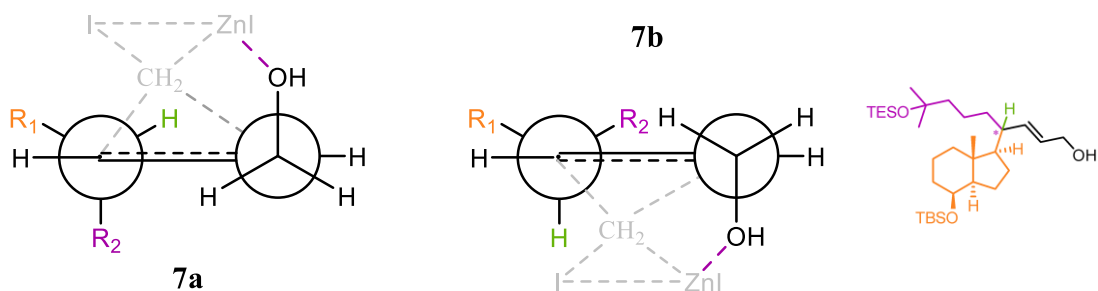
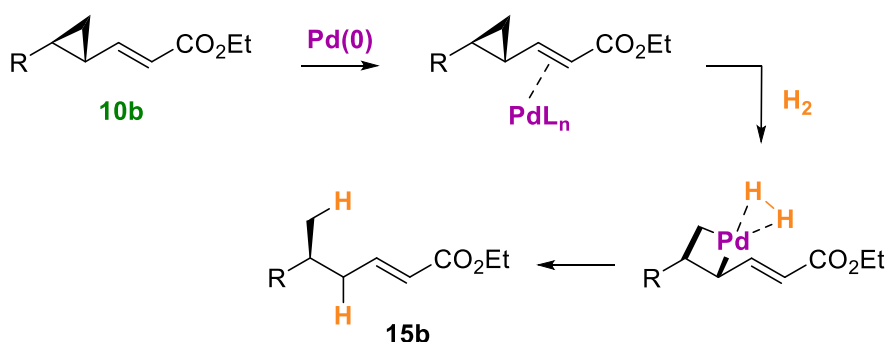


Figure 3. Newman projections of cyclopropanation reaction of more stable conformation of **7a** and **7b** that illustrate the stereoselectivity of reaction.

TPAP oxidation of **8a/8b** gave 95%/92% yield of aldehydes **9a/9b** which underwent the Wittig reaction to afford esters **10a/10b** in 99%/99% yield.

Under the usual hydrogenation conditions with 10% Pd/C in hexane at normal pressure and room temperature, ester **10b** afforded **15b** and **11b** as an inseparable mixture. The mechanism of the regioselective reductive ring opening of vinylcyclopropane induced by palladium on activated carbon is shown in **Scheme 4**.



Scheme 4. Regioselective ring opening of vinylcyclopropane **10b** by hydrogenation with Pd on activated carbon.

Given the apparent failure of catalytic hydrogenation, we try the Cu(I)-catalyzed 1,4-hydrosilylation of α,β -unsaturated ester **10a/10b**. Achiral phosphine-copper hydride complexes ($[(\text{Ph}_3\text{P})\text{CuH}]_6$) have been shown to act as catalysts for conjugate reductions of α,β -unsaturated carbonyl compounds in combination with stoichiometric polymethylhydrosiloxane (PMHS).¹⁹ Then, under this methodology saturated esters **11a/11b** were obtained in 93%/95% yield.

Treatment of saturated esters **11a/11b** with MeLi afforded the corresponding alcohols **12a/12b**. TBAF deprotection of the hydroxyl groups of **12a/12b**, followed by a PDC oxidation and trimethylsilyl protection of the side chain hydroxyl groups afforded target Grundmann ketones **3a/3b** in 68%/68% overall yield (4 steps).

We were delighted to see that compound **13b** could be recrystallized from a mixture of AcOEt:CH₂Cl₂ (1:1), hence its structure could be confirmed unambiguously by X-Ray crystallographic analysis as shown in Figure 4.

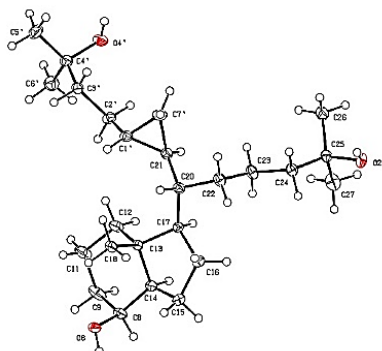
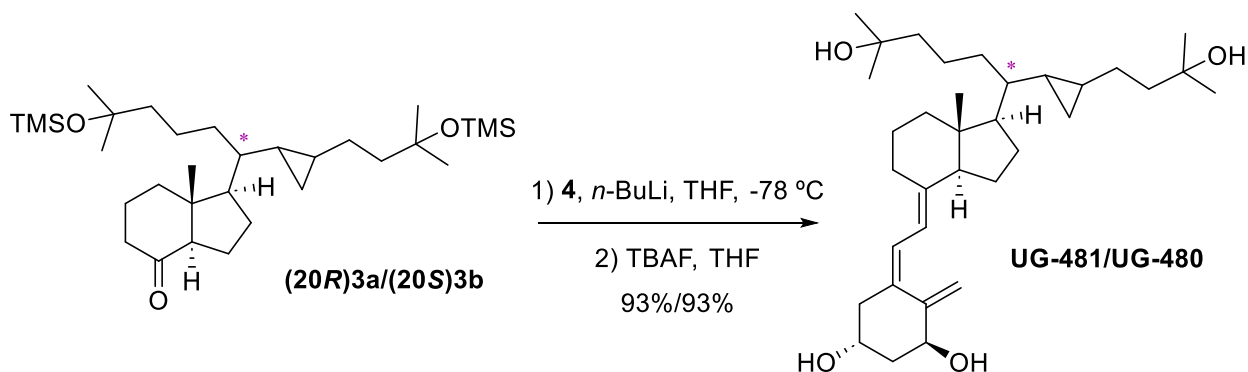


Figure 4. ORTEP plot of the X-Ray single crystal structure of triol **13b**.

With ketones **3a/3b** in hand, the stage was now set for the Wittig-Horner reaction with phosphine oxide **4** and the final desilylation to afford uneventfully 93%/93% yield of the target Gemini compounds **UG-481** and **UG-480** (Scheme 5).



Scheme 5. Preparation of **UG-480** and **UG-481**.

Biological Evaluation. The antiproliferative effects of the analogues **UG-480** and **UG-481** were assessed in estrogen receptor positive MCF-7 breast adenocarcinoma cells (Figure 5). The antiproliferative activity of **UG-480** was comparable to that of 1,25(OH)₂D₃, whereas the analogue **UG-481** was less active. Indeed, treatment with 10⁻⁸ M **UG-481** did not decrease proliferation of MCF-7 cells, whereas incubation with 10⁻⁸ M **UG-480** or 1,25(OH)₂D₃ resulted in a reduction of approximately 25% in cell proliferation. Higher concentrations of **UG-481** did reduce MCF-7 cell proliferation when compared to vehicle-stimulated cells but to a lesser extent than similar concentrations of 1,25(OH)₂D₃ or **UG-480**. Thus, in agreement with previously published data, the 17,20 threo (20S) compound is more active than the 17,20-erythro one.^{17,20}

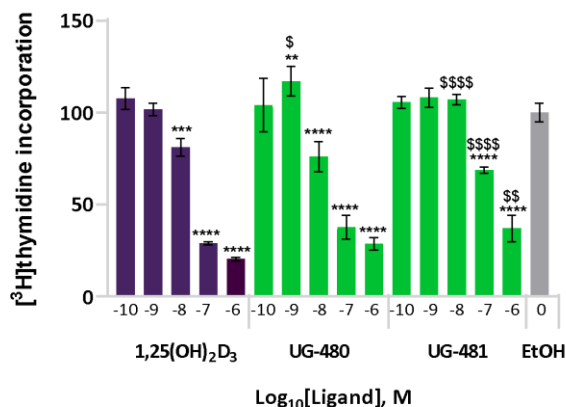


Figure 5. Anti-proliferative effects of **UG-480** and **UG-481**. Human breast adenocarcinoma MCF-7 cells were treated for 72 h with increasing doses of 1,25(OH)₂D₃, **UG-480**, or **UG-481**, after which [³H]thymidine incorporation was measured. ** p < 0.01, *** p < 0.001; **** p < 0.0001 versus vehicle treatment. \$ p < 0.05, \$\$ p < 0.01, \$\$\$\$ p < 0.0001 versus the same concentration of 1,25(OH)₂D₃.

Molecular modelling studies. Docking assays showed that both **UG-480** and **UG-481** resulted in a unique lowest energy cluster of conformations, with comparable docked energies being calculated. For **UG-480** a docked energy of -17.11 Kcal/mol was found, while **UG-481** exhibited an energy of -19.41 Kcal/mol. Both values were found to be lower to that calculated for calcitriol (-15.53 Kcal/mol) and similar to that observed for **UVB1** (-20.01 Kcal/mol). **Figure 6** presents a superimposed view of the binding modes of **UG-480** and **UG-481** with the dihydroxycyclohexyl rings being superimposed in both docked poses. Both ligands show an almost identical interaction pattern (**Figure S1**).

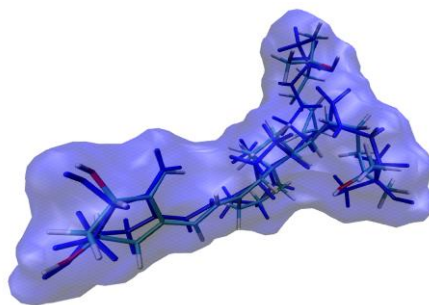


Figure 6. Binding mode of **UG-480** (blue) and **UG-481** (colored) in the 1DB1 X-ray structure.

However, a subtle difference is observed with respect to the positioning of the side chains including the cyclopropane ring of both ligands (**Figure S2**). In the case of **UG-480**, the pharmacophoric contact with His305 and His397 is accomplished by the hydroxyl group opposed to the chain containing the cyclopropane ring, while **UG-481** establishes this contact through the hydroxyl located in the chain containing the cyclopropane ring. In order to further study the pharmacodynamic consequences of these differential binding modes, molecular dynamics (MD) simulations were carried out.

Molecular dynamics studies. Both complexes were subjected to explicit solvent MD simulations, with their corresponding trajectories being afterwards analyzed in terms of trajectory stability and convergence. In particular, hydrogen bonding distance between the ligand and His305 and His397 was tracked (**Figure 7**).

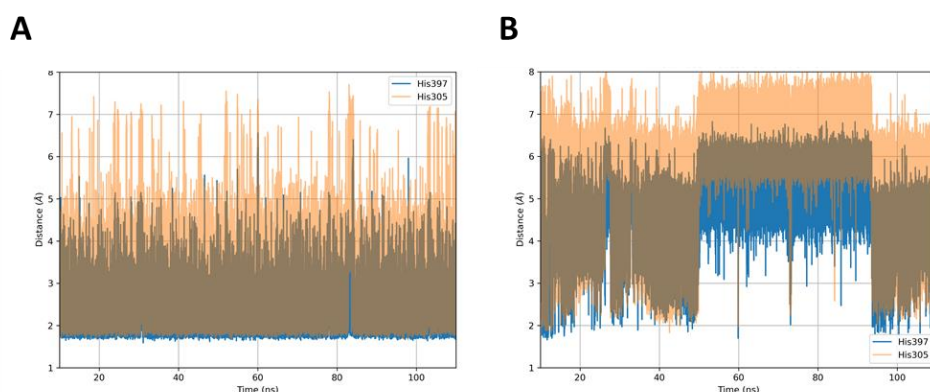


Figure 7. Distances between the pharmacophoric residues His305 and His397 and **UG-480** (A) and **UG-481** (B) during MD simulations.

The pharmacophoric contacts between **UG-480** and His305 and His397 are maintained throughout the simulated trajectory (**Figure 7A**), while **UG-481** was only able to maintain the interaction with His397 (**Figure 7B**). This feature strongly suggests that presence of the cyclopropane ring in the chain bearing the interacting hydroxyl moiety introduces a certain extent of conformational restriction that prevents the simultaneous geometric optimization of the two hydrogen bonds with His305 and His397.

To further evaluate the overall interaction pattern between VDR and **UG-480** and **UG-481**, the complete interactions fingerprint was computed by applying a per-residue decomposition of the corresponding free-energy of interaction with individual analyses corresponding to the Van der Waals (**Figure 8A**) and electrostatic (**Figure 8B**) components.

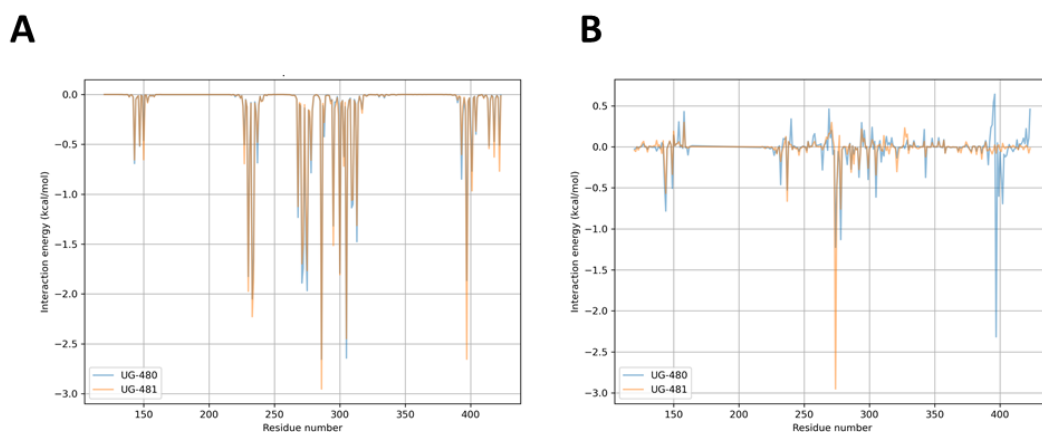


Figure 8. Superimposed interaction fingerprints calculated for **UG-480** and **UG-481**: (A) Van der Waals (VDW) and (B) electrostatic (ELE) components.

Similar interaction profiles are observed when the VDW component is analyzed, while on the other hand significant differences are found for the ELE interaction components of **UG-480** and **UG-481**. Noteworthy, **UG-480** is able to establish a sustained

electrostatic interaction with residue His397, which as mentioned before constitutes an already reported pharmacophoric contact. In contrast, **UG-481** is not able to establish such interaction with His397, but in this case a strong interaction is observed with residue Arg274. The total interaction energy profiles accounting for gas phase interactions as well as solvation effects, are presented in **Figure S3**, showing that the interaction of **UG-480** with residue His397 is energetically favored.

Overall, molecular docking and molecular dynamics simulations suggests that **UG-480** may exhibit a more efficient VDR mediated bioactivity compared to that of **UG-481**, since it is able to strongly interact through stable hydrogen bond interactions with the pharmacophoric residue His397.

Crystal structures of VDR complexes. We crystalized the two analogs **UG-480** and **UG-481** in complex with zebrafish zVDR ligand binding domain (LBD) and NCoA2 coactivator peptide. The structures of the VDR/**UG-480** and VDR/**UG-481** complexes were refined at a resolution of 2.56 and 3.01 Å, respectively. The complexes adopt the canonical, active conformation, characteristic of all previously reported agonist-bound nuclear receptor LBDs. Compared with the structure of the zVDR LBD/Gemini and zVDR LBD/1,25(OH)₂D₃ complexes, the atomic coordinates of all C α atoms of zVDR bound to **UG-480** show root mean square deviations of 0.25 Å and 0.27 Å, respectively. The atomic coordinates of all C α atoms of zVDR bound to **UG-481** compared to the zVDR LBD-Gemini and zVDR LBD/1,25(OH)₂D₃ complexes, show root mean square deviations of 0.28 Å and 0.28 Å, respectively. Similarly, to the previously described crystal structures of VDR complexes with gemini ligands (20-23), the accommodation of the second side chain of **UG-480** and **UG-481** induce a backbone shift of the highly flexible H6-H7 region of VDR (**Figure 9A and Supplementary 4A**). In contrast to gemini ligands with modified side chain that preferentially occupied the parental channel occupied by the aliphatic side chain of 1,25(OH)₂D₃,^{20,23} the modified second side chains of **UG-480** and **UG-481** occupy the secondary channel (**Figure 9A and Figure S4**). However, the density of the modified side chain of **UG-481**, is only partial indicating that it is more flexible and less well accommodated (**Figure S5**). For both ligands, as a consequence of the increased rigidity of the cyclopropane group and longer side chain, a larger shift of loop 6-7 and beginning of H7 is observed compared to the parental Gemini. In comparison to 1,25(OH)₂D₃, the C α atoms of residues zLeu335, zGlu336, zLeu337 of VDR/**UG-480** complex, are being shifted by 2.7, 3.8 and 2.8 Å outwards, respectively. For VDR/**UG-481**, the C α atoms of residues zLeu335, zGlu336, zLeu337 are being shifted by 2.5, 3.4 and 2.5 Å outwards. The same atoms in VDR/Gemini complex are shifted by 1.3, 2.4 and 1.9 Å outwards, respectively. These shifts are accompanied by rearrangements of some side chains atoms, notably those of zGlu336 and zLeu337.

The A, seco-B, C, and D rings present conformations similar to those observed in the presence of the natural ligand. The interactions between the A, seco-B and C/D rings of both ligands with the receptor are identical to those of the natural ligand and the hydroxyl groups of the A ring form similar hydrogen bonds as 1,25(OH)₂D₃ or Gemini. The hydroxyl group of the non-modified side chain of **UG-480** that occupies the parental pocket forms hydrogen bond with His423 only and a weaker interaction with zHis333 due to the accommodation of the second modified chain and conformational changes that destabilize zHis333 (**Figure 9B**). The hydroxyl group of the non-modified side chain of **UG-481** forms hydrogen bonds with both zHis 333 and zHis423 (**Figure S4B**). For both ligands, the hydroxyl group of the modified longer side chain does not form any hydrogen bond. The interactions of the aliphatic side chain of **UG-480** occupying the canonical pocket forms similar interactions as 1,25(OH)₂D₃, expect some differential interactions

with zHis333. The aliphatic side chain of **UG-481** occupying the canonical pocket forms weaker interactions with C-terminal residue zPhe448. Due to the uncertainty of the position of the modified side chain of **UG-481**, we will only describe the interactions formed by the modified second side chain of **UG-480** that is oriented towards helix H7 and the end of H10 and forms additional/increased hydrophobic interactions in comparison to 1,25(OH)₂D₃, with zMet300, zLeu337, zLeu338, zLeu341, zLeu419 and zGlu422 (**Figure 9B**). In addition, the cyclopropane group of **UG-480** forms specific interactions with zHis333 and zHis423. The additional contacts of the modified side chain compensate the weaker/loss of hydrogen bonds with the two histidines.

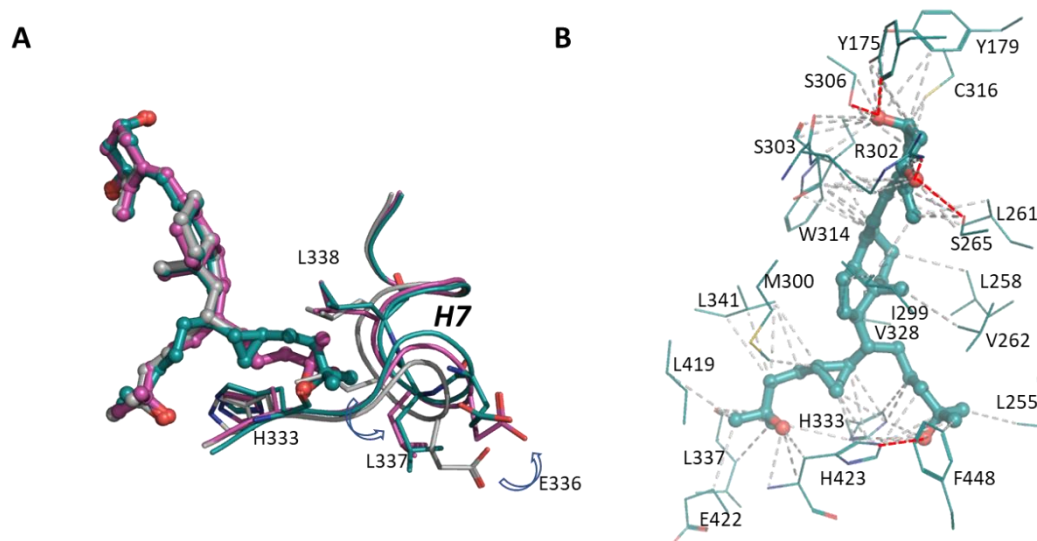


Figure 9. Crystal structure of VDR complex with **UG-480** (PDB: 9EYR). (A) Adaptability of the ligand binding pocket (LBP). Superimposition of **UG-480** (blue), Gemini (pink) and 1,25(OH)₂D₃ (grey) bound to zVDR. The most differing region H7 is shown as ribbon and side chain residues that show conformational changes are indicated. (B) Details of interactions between zVDR LBP and **UG-480**. Hydrophobic and van der Waals interactions (grey), and hydrogen bonds (red) are displayed at 4.0 Å cut-off (dotted lines).

CONCLUSION

In summary, we described the synthesis of two new Gemini analogues that incorporated a modified longer side chain containing a cyclopropane group. The evaluation of the bioactivities of these two analogues indicated that the 17,20 threo (20S) compound, **UG-480**, is the more active one and as active as 1,25(OH)₂D₃. Docking and MD data showed that the compounds bind efficiently to VDR with **UG-480** forming an energetically more favorable interaction with His397. Structural analysis indicated that whereas the **UG-480** compound efficiently stabilizes the active VDR conformation, it induces conformational changes in H6-H7 VDR region larger than the changes induced by the parental Gemini and that is due to the occupancy of the secondary channel by the modified side chain. The additional interactions formed by the modified side chain and cyclopropane group, contribute to the stabilization of the active conformation.

EXPERIMENTAL SECTION

Chemistry. Solvents were purified and dried by standard procedures before use. Melting points are uncorrected. ^1H NMR and ^{13}C NMR spectra were recorded with a Bruker ARX-400 spectrometer (400 MHz for ^1H NMR, 100.61 MHz for ^{13}C NMR) using TMS as internal standard (chemical shifts in δ values, J in Hz). Flash chromatography (FC) was performed on silica gel (Merck 60, 230-400 mesh); analytical TLC was performed on plates precoated with silica gel (Merck 60 F254, 0.25mm). Mass spectra (FAB, EI) were recorded using FISIONS VG and electron spray ionization (ESI-MS) spectroscopy was recorded using Bruker FTMS APEXIII. Optical rotations were obtained using a Jasco P-2000 polarimeter. IR spectra were recorded on a JASCO FT/I(R)-6100 spectrophotometer. The purity of the final compounds was assessed HPLC-DAD equipped with a UV-1 absorbance detector 254 nm and a silica column (250x4.6 mm, 5 μm particle size; Isopropanol/hexanes 10:90; Flow rate = 4 mL/min), and was identified as >95%.

(8 β)-(20S)-Des-A,B-8-[(*tert*-butyldimethyl)silyloxy]-20-(4'-hydroxy-4'-methylpentyl)pregn-21-al (5a) and (8 β)-(20R)-Des-A,B-8-[(*tert*-butyldimethyl)silyloxy]-20-(4'-hydroxy-4'-methylpentyl)pregn-21-al (5b): To a solution of **1a/1b** (780 mg, 1.88 mmol, 1.0 equiv.) in dry CH_2Cl_2 (22 mL) at rt was added BAIB (913 mg, 2.83 mmol, 1.5 equiv.), TEMPO (44 mg, 0.28 mmol, 15 mol%) and the solution was stirred at this temperature for 19 h. The solvent was removed *in vacuo* and the crude material was dissolved in $t\text{-BuOMe}$ (15 mL) and washed with 10% w/v aq. $\text{Na}_2\text{S}_2\text{O}_3$ solution (2 x 15 mL) and sat. aq. NaHCO_3 solution (2 x 15 mL). The organic phase was dried over Na_2SO_4 , filtered and concentrated *in vacuo*. The residue was chromatographed on silicagel using 20% EtOAc/hexane as eluent, affording the product as a colorless oil (737 mg, 95%)/(737 mg, 95%). Compound **5a**: $^1\text{H-NMR}$ (400 MHz, CDCl_3): δ 9.46 (d, $J = 4.7$ Hz, 1H, CHO), 3.99 (q, $J = 2.7$ Hz, 1H, H-8), 2.31 - 2.24 (m, 1H, H-20), 1.89 - 1.84 (m, 1H), 1.82 - 1.73 (m, 1H), 1.70 - 1.63 (m, 3H), 1.60 - 1.45 (m, 5H), 1.40 - 1.20 (m, 9H), 1.15 (s, 6H, $\text{CH}_3\text{-}5'$, $\text{CH}_3\text{-}6'$), 0.92 (s, 3H, $\text{CH}_3\text{-}18$), 0.85 (s, 9H, $\text{CH}_3\text{-}^t\text{Bu}$), -0.02 (s, 3H, $\text{CH}_3\text{-Si}$), -0.03 (s, 3H $\text{CH}_3\text{-Si}$); $^{13}\text{C-NMR}$ (101 MHz, CDCl_3): δ 205.6 (CHO), 70.8 (C-4'), 69.1 (CH-8), 54.5 (CH-20), 52.6 (CH-17), 50.0 (CH-14), 43.9 (CH_2), 42.7 (C-13), 40.6 (CH_2), 34.4 (CH_2), 29.3 ($\text{CH}_3\text{-}5'/6'$), 29.3 ($\text{CH}_3\text{-}5'/6'$), 28.7 (CH_2), 25.9 ($\text{CH}_3\text{-}^t\text{Bu}$), 25.8 (CH_2), 23.3 (CH_2), 22.0 (CH_2), 18.1 (C- ^tBu), 17.7 (CH_2), 14.6 ($\text{CH}_3\text{-}18$), -4.7 ($\text{CH}_3\text{-Si}$), -5.1 ($\text{CH}_3\text{-Si}$); **IR** (ATR, cm^{-1}): ν 3429, 2948, 2929, 2856, 1723, 1471, 1376, 1252, 1165, 1084, 1031, 836, 774; **MS** (ESI): m/z (%) 393.3 ([M - OH] $^+$, 100), 261.2 ([M - OH - TBSOH] $^+$, 10); **HRMS** (ESI): m/z calculated for $\text{C}_{24}\text{H}_{45}\text{O}_2\text{Si}$ [M - OH] $^+$ 393.3183, found 393.3177; **TLC** (SiO_2 ; 50% EtOAc/hexane): $R_f = 0.76$. Compound **5b**: $^1\text{H-NMR}$ (400 MHz, CDCl_3): δ 9.43 (d, $J = 4.7$ Hz, 1H, CHO), 3.97 (q, $J = 2.7$ Hz, 1H, H-8), 2.26 - 2.12 (m, 1H, H-20), 1.86 - 1.75 (m, 1H), 1.73 - 1.62 (m, 2H), 1.57 - 1.51 (m, 3H), 1.48 - 1.51 (m, 3H), 1.38 - 1.17 (m, 9H), 1.14 (s, 6H, $\text{CH}_3\text{-}5'$, $\text{CH}_3\text{-}6'$), 0.88 (s, 3H, $\text{CH}_3\text{-}18$), 0.84 (s, 9H, $\text{CH}_3\text{-}^t\text{Bu}$), -0.03 (s, 3H, $\text{CH}_3\text{-Si}$), -0.04 (s, 3H, $\text{CH}_3\text{-Si}$); $^{13}\text{C-NMR}$ (101 MHz, CDCl_3): δ 206.3 (CHO), 70.8 (C-4'), 69.1 (CH-8), 54.5 (CH-20), 52.6 (CH-17), 51.5 (CH-14), 43.8 (CH_2), 41.9 (C-13), 39.4 (CH_2), 34.4 (CH_2), 29.3 ($\text{CH}_3\text{-}5'/6'$), 29.2 ($\text{CH}_3\text{-}5'/6'$), 28.9 (CH_2), 26.0 ($\text{CH}_3\text{-}^t\text{Bu}$), 25.9 (CH_2), 22.6 (CH_2), 22.0 (CH_2), 18.1 (C- ^tBu), 17.4 (CH_2), 14.8 ($\text{CH}_3\text{-}18$), -4.7 ($\text{CH}_3\text{-Si}$), -5.1 ($\text{CH}_3\text{-Si}$); **IR** (ATR, cm^{-1}): ν 3408, 2929, 2903, 2856, 1722, 1471, 1377, 1252, 1166, 1085, 1027, 851, 774; **MS** (ESI): m/z (%) 393.3 ([M - OH] $^+$, 100), 261.2 ([M - OH - TBSOH] $^+$, 17); **HRMS** (ESI): m/z calculated for $\text{C}_{24}\text{H}_{46}\text{NaO}_3\text{Si}$ [M + Na] $^+$ 433.3108, found 433.3120; **TLC** (SiO_2 ; 50% EtOAc/hexane): $R_f = 0.76$.

(22E)-(8β)-(20R)-Des-A,B-8-[(tert-butyldimethyl)silyloxy]-21-(3'-hydroxy-3'-methylbutyl)cholan-24-oate (6a) and (22E)-(8β)-(20S)-Des-A,B-8-[(tert-butyldimethyl)silyloxy]-21-(3'-hydroxy-3'-methylbutyl)cholan-24-oate (6b): To a solution of **5a/5b** (790 mg, 1.92 mmol, 1.0 equiv.) in anhydrous THF (22 mL) at rt was added triphenylcarbethoxymethylenephosphorane (6.6 g, 19.23 mmol, 10.0 equiv.) and the solution was stirred at 60 °C for 7 days. Then the mixture was allowed to reach rt and the solvent was removed *in vacuo*. The residue was chromatographed on silicagel using 10% EtOAc/hexane as eluent, affording the product as a colorless oil (777 mg, 84%)/(888 mg, 96%). Compound **6a**: ¹H-NMR (400 MHz, CDCl₃): δ 6.60 (dd, *J* = 15.5, 10.2 Hz, 1H, H-22), 5.67 (d, *J* = 15.5 Hz, 1H, H-23), 4.12 (q, *J* = 7.1 Hz, 2H, CH₂-OEt), 3.94 (q, *J* = 2.8 Hz, 1H, H-8), 2.16 – 2.08 (m, 1H, H-20), 1.90 – 1.84 (m, 1H), 1.78 – 1.72 (m, 1H), 1.67 – 1.58 (m, 3H), 1.56 – 1.39 (m, 4H), 1.37 – 1.18 (m, 12H), 1.12 (s, 6H, CH₃-4', CH₃-5'), 0.89 (s, 3H, CH₃-18), 0.83 (s, 9H, CH₃-^tBu), -0.04 (s, 3H, CH₃-Si), -0.06 (s, 3H, CH₃-Si); ¹³C-NMR (101 MHz, CDCl₃): δ 166.7 (C=O), 153.0 (CH-22), 120.5 (CH-23), 70.7 (C-3'), 69.2 (CH-8), 60.0 (CH₂-OEt), 53.5 (CH-17), 52.9 (CH-14), 45.1 (CH-20), 43.8 (CH₂), 42.4 (C-13), 40.6 (CH₂), 34.3 (CH₂), 33.0 (CH₂), 29.2 (CH₃-4'/5'), 29.1 (CH₃-4'/5'), 27.2 (CH₂), 25.7 (CH₃-^tBu), 22.8 (CH₂), 21.8 (CH₂), 17.9 (C-^tBu), 17.6 (CH₂), 14.2 (CH₃-18, CH₃-OEt), -4.9 (CH₃-Si), -5.3 (CH₃-Si); IR (ATR, cm⁻¹): ν 3432, 2951, 2930, 2856, 1720, 1650, 1471, 1368, 1250, 1164, 1031, 836, 774; MS (ESI): *m/z* (%) 503.4 ([M + Na]⁺, 66), 463.4 ([M - OH]⁺, 100), 331.3 ([M - OH - TBSOH]⁺, 15); HRMS (ESI): *m/z* calculated for C₂₈H₅₂NaO₄Si [M + Na]⁺ 503.3527, found 503.3526; TLC (SiO₂; 30% EtOAc/hexane): R_f = 0.54. Compound **6b**: ¹H-NMR (400 MHz, CDCl₃): δ 6.68 (dd, *J* = 15.7, 10.5 Hz, 1H, H-22), 5.72 (d, *J* = 15.7 Hz, 1H, H-23), 4.25 – 4.08 (m, 2H, CH₂-OEt), 3.96 (q, *J* = 2.7, 2.5 Hz, 1H, H-8), 2.16 – 2.03 (m, 1H, H-20), 2.88 – 2.79 (m, 1H), 1.70 – 1.60 (m, 3H), 1.53 – 1.38 (m, 4H), 1.35 – 1.21 (m, 12H), 1.16 (s, 6H, CH₃-4', CH₃-5'), 1.07 – 0.89 (m, 2H), 0.85 (s, 12H, CH₃-18, CH₃-^tBu), -0.02 (s, 3H, CH₃-Si), -0.03 (s, 3H, CH₃-Si); ¹³C-NMR (101 MHz, CDCl₃): δ 166.8 (C=O), 154.1 (CH-22), 120.6 (CH-23), 71.0 (C-3'), 69.3 (CH-8), 60.2 (CH₂-OEt), 55.0 (CH-17), 52.9 (CH-14), 45.5 (CH-20), 43.9 (CH₂), 42.2 (C-13), 39.7 (CH₂), 34.5 (CH₂), 33.5 (CH₂), 29.4 (CH₃-4'/5'), 29.2 (CH₃-4'/5'), 26.9 (CH₂), 25.8 (CH₃-^tBu), 22.9 (CH₂), 21.5 (CH₂), 18.1 (C-^tBu), 17.5 (CH₂), 14.4 (CH₃-18/CH₃-OEt), 14.1 (CH₃-18/CH₃-OEt), -4.7 (CH₃-Si), -5.1 (CH₃-Si); IR (ATR, cm⁻¹): ν 3462, 2949, 2932, 2856, 1720, 1650, 1471, 1368, 1251, 1165, 1083, 1032, 851, 774; MS (ESI): *m/z* (%) 503.4 ([M + Na]⁺, 83), 463.4 ([M - OH]⁺, 100), 331.3 ([M - OH - TBSOH]⁺, 27); HRMS (ESI): *m/z* calculated for C₂₈H₅₂NaO₄Si [M + Na]⁺ 503.3527, found 503.3520; TLC (SiO₂; 30% EtOAc/hexane): R_f = 0.54.

Ethyl (22E)-(8β)-(20R)-des-A,B-8-[(tert-butyldimethyl)silyloxy]-21-(3'-[(triethyl)silyloxy]-3'-methylbutyl)cholan-22-en-24-oate (2a) and Ethyl (22E)-(8β)-(20S)-des-A,B-8-[(tert-butyldimethyl)silyloxy]-21-(3'-[(triethyl)silyloxy]-3'-methylbutyl)cholan-22-en-24-oate (2b): To a solution of **6a/6b** (720 mg, 1.49 mmol, 1.0 equiv.) in dry CH₂Cl₂ (14 mL) at 0 °C was added 2,6-lutidine (1.6 mL, 14.97 mmol, 10.0 equiv.), TESOTf (507 μL, 2.24 mmol, 1.5 equiv.) dropwise and the solution was stirred at rt for 3 h. The mixture reaction was quenched with sat. aq. NaHCO₃ solution (15 mL) and the layers were separated. The aqueous phase was extracted with CH₂Cl₂ (3 x 15 mL) and the combined organic extracts were dried over Na₂SO₄, filtered and concentrated *in vacuo*. The residue was chromatographed on silicagel using 1.5% EtOAc/hexane as eluent, affording the product as a colorless oil (847 mg, 95%)/(847 mg, 95%). Compound **2a**: ¹H-NMR (400 MHz, CDCl₃): δ 6.64 (dd, *J* = 15.6, 10.2 Hz, 1H, H-22), 5.69 (d, *J* = 15.6 Hz, 1H, H-23), 4.15 (q, *J* = 7.1 Hz, 2H, CH₂-OEt), 3.97 (q, *J* =

2.7 Hz, 1H, H-8), 2.19 – 2.08 (m, 1H, H-20), 1.97 – 1.88 (m, 1H), 1.85 - 1.73 (m, 1H), 1.68 – 1.46 (m, 4H), 1.44 – 1.29 (m, 6H), 1.28 – 1.22 (m, 6H), 1.20 – 1.16 (m, 2H), 1.14 (s, 3H, CH₃-4'/5'), 1.13 (s, 3H, CH₃-4'/5'), 0.94 – 0.88 (m, 12H, CH₃-18, CH₃-TES), 0.87 (s, 9H, CH₃-^tBu), 0.52 (q, *J* = 7.7 Hz, 6H, CH₂-TES), -0.01 (s, 3H, CH₃-Si), -0.03 (s, 3H, CH₃-Si); ¹³C-NMR (101 MHz, CDCl₃): δ 166.9 (C=O), 153.3 (CH-22), 120.6 (CH-23), 73.3 (C-3'), 69.4 (CH-8), 60.1 (CH₂-OEt), 53.8 (CH-17), 53.2 (CH-14), 45.4 (CH-20), 45.1 (CH₂), 42.6 (C-13), 40.9 (CH₂), 34.5 (CH₂), 33.2 (CH₂), 30.2 (CH₃-4'/5'), 29.8 (CH₃-4'/5'), 27.4 (CH₂), 25.9 (CH₃-^tBu), 23.0 (CH₂), 22.0 (CH₂), 18.1 (C-^tBu), 17.8 (CH₂), 14.4 (CH₃-18/CH₃-OEt), 14.3 (CH₃-18/CH₃-OEt), 7.2 (CH₃-TES), 6.9 (CH₂-TES), -4.7 (CH₃-Si), -5.1 (CH₃-Si); **IR** (ATR, cm⁻¹): ν 2956, 2925, 2854, 1724, 1652, 1463, 1365, 1252, 1163, 1033, 836, 775; **MS** (ESI): *m/z* (%) 595.5 ([M + H]⁺, 32), 463.4 ([M - OTEs]⁺, 100); **HRMS** (ESI): *m/z* calculated for C₃₄H₆₆NaO₄Si₂ [M + Na]⁺ 617.4392, found 617.4392; **TLC** (SiO₂; 10% EtOAc/hexane): R_f = 0.73. **Compound 2b**: ¹H-NMR (400 MHz, CDCl₃): δ 6.69 (dd, *J* = 15.6, 10.5 Hz, 1H, H-22), 5.71 (d, *J* = 15.6 Hz, 1H, H-23), 4.21 – 4.14 (m, 2H, CH₂-OEt), 3.98 (q, *J* = 2.8 Hz, 1H, H-8), 2.13 – 2.03 (m, 1H, H-20), 1.90 – 1.76 (m, 1H), 1.72 – 1.62 (m, 3H), 1.57 - 1.42 (m, 2H), 1.40 – 1.24 (m, 12H), 1.22 – 1.18 (m, 1H), 1.15 (s, 3H, CH₃-4'/5'), 1.14 (s, 3H, CH₃-4'/5'), 0.91 (t, *J* = 7.9 Hz, 9H, CH₃-TES), 0.88 – 0.84 (m, 12H, CH₃-18, CH₃-^tBu), 0.53 (q, *J* = 7.6 Hz, 6H, CH₂-TES), -0.01 (s, 3H, CH₃-Si), -0.02 (s, 3H, CH₃-Si); ¹³C-NMR (101 MHz, CDCl₃): δ 166.8 (C=O), 154.3 (CH-22), 120.5 (CH-23), 73.4 (C-3'), 69.4 (CH-8), 60.1 (CH₂-OEt), 55.1 (CH-17), 52.9 (CH-14), 45.7 (CH-20), 45.1 (CH₂), 42.2 (C-13), 39.8 (CH₂), 34.6 (CH₂), 33.6 (CH₂), 30.2 (CH₃-4'/5'), 29.8 (CH₃-4'/5'), 27.0 (CH₂), 25.9 (CH₃-^tBu), 22.9 (CH₂), 21.6 (CH₂), 18.1 (C-^tBu), 17.6 (CH₂), 14.4 (CH₃-18/CH₃-OEt), 14.1 (CH₃-18/CH₃-OEt), -4.7 (CH₃-Si), -5.1 (CH₃-Si); **IR** (ATR, cm⁻¹): ν 2952, 2933, 2875, 2856, 1721, 1652, 1462, 1365, 1252, 1166, 1034, 837, 775; **MS** (ESI): *m/z* (%) 595.5 ([M + H]⁺, 20), 463.4 ([M - OTEs]⁺, 100); **HRMS** (ESI): *m/z* calculated for C₃₄H₆₇O₄Si₂ [M + H]⁺ 595.4572, found 595.4564; **TLC** (SiO₂; 10% EtOAc/hexane): R_f = 0.73.

(22E)-(8β)-(20R)-Des-A,B-8-[(*tert*-butyldimethyl)silyloxy]-21-(3'-[(triethyl)silyloxy]-3'-methylbutyl)cholan-22-en-24-ol (7a) and (22E)-(8β)-(20S)-Des-A,B-8-[(*tert*-butyldimethyl)silyloxy]-21-(3'-[(triethyl)silyloxy]-3'-methylbutyl)cholan-22-en-24-ol (7b): To a solution of **2a/2b** (840 mg, 1.41 mmol, 1.0 equiv.) in anhydrous THF (16 mL) at -78 °C was added DIBAL-H (1.0 M in hexane, 4.2 mL, 4.23 mmol, 3.0 equiv.) dropwise and the solution was stirred at this temperature for 1 h and after was worked up according to Fieser procedure. Then the mixture was allowed to warm up to rt and was added ^tBuOMe (10 mL), H₂O (3 mL) and the mixture was left standing until the formation of a translucent gel. Subsequently, was added 4.0 M aq. NaOH solution (3 mL), H₂O (7.5 mL) and the mixture was left standing until the formation of white solid. The solvent was dried over Na₂SO₄, filtered and concentrated *in vacuo*. The residue was chromatographed on silicagel using 4% EtOAc/hexane as eluent, affording the product as a colorless oil (730 mg, 94%)/(738 mg, 95%). **Compound 7a**: ¹H-NMR (400 MHz, CDCl₃): δ 5.53 (dt, *J* = 15.3, 6.1 Hz, 1H, H-23), 5.33 (ddt, *J* = 15.3, 9.5, 1.3 Hz, 1H, H-22), 4.05 (d, *J* = 6.1 Hz, 2H, CH₂-24), 4.01 (q, *J* = 2.9 Hz, 1H, H-8), 2.02 - 1.91 (m, 2H), 1.86 - 1.73 (m, 1H), 1.69 - 1.64 (m, 1H), 1.61 - 1.46 (m, 3H), 1.45 - 1.17 (m, 12H), 1.16 (s, 3H, CH₃-4'/5'), 1.15 (s, 3H, CH₃-4'/5'), 1.12 - 1.09 (m, 1H), 0.96 - 0.90 (m, 12H, CH₃-18, CH₃-TES), 0.88 (s, 9H, CH₃-^tBu), 0.57 (q, *J* = 8.2 Hz, 6H, CH₂-TES), 0.00 (s, 3H, CH₃-Si), -0.01 (s, 3H, CH₃-Si); ¹³C-NMR (101 MHz, CDCl₃): δ 137.5 (CH-22), 128.2 (CH-23), 73.4 (C-3'), 69.5 (CH-8), 63.9 (CH₂-24), 54.3 (CH-17), 53.3 (CH-14), 45.1 (CH-20), 45.0 (CH₂), 42.2 (C-13), 40.8 (CH₂), 34.5 (CH₂), 33.8 (CH₂),

30.1 (CH₃-4'/5'), 29.7 (CH₃-4'/5'), 27.6 (CH₂), 25.8 (CH₃-^tBu), 22.9 (CH₂), 21.8 (CH₂), 18.0 (C-^tBu), 17.7 (CH₂), 14.2 (CH₃-18), 7.1 (CH₃-TES), 6.8 (CH₂-TES), -4.8 (CH₃-Si), -5.2 (CH₃-Si); **IR** (ATR, cm⁻¹): ν 3304, 2956, 2924, 2871, 2853, 1463, 1377, 1252, 1164, 1085, 1032, 1004, 971, 836, 774, 722; **MS** (ESI): *m/z* (%) 575.4 ([M + Na]⁺, 15), 403.4 ([M - OH - TBSOH]⁺, 100); **HRMS** (ESI): *m/z* calculated for C₃₂H₆₄NaO₃Si₂ [M + Na]⁺ 575.4286, found 585.4286; **TLC** (SiO₂; 20% EtOAc/hexane): R_f = 0.59. Compound **7b**: **¹H-NMR** (400 MHz, CDCl₃): δ 5.50 (dt, *J* = 15.5, 5.8 Hz, 1H, H-23), 5.37 – 5.31 (m, 1H, H-22), 4.08 (d, *J* = 5.9 Hz, 2H, CH₂-24), 3.97 (q, *J* = 2.9 Hz, 1H, H-8), 1.98 - 1.88 (m, 1H, H-20), 1.83 - 1.62 (4H, m), 1.55 - 1.48 (m, 1H), 1.41 - 1.21 (m, 12H), 1.16 (s, 3H, CH₃-4'/5'), 1.15 (s, 3H, CH₃-4'/5'), 1.09 - 1.01 (m, 2H), 0.95 - 0.90 (m, 12H, CH₃-18, CH₃-TES), 0.87 (s, 9H, CH₃-^tBu), 0.54 (q, *J* = 7.8 Hz, 6H, CH₂-TES), -0.02 (s, 3H, CH₃-Si), -0.02 (s, 3H, CH₃-Si); **¹³C-NMR** (101 MHz, CDCl₃): δ 137.9 (CH-22), 128.2 (CH-23), 73.6 (C-3'), 69.4 (CH-8), 64.0 (CH₂-25), 55.2 (CH-17), 53.1 (CH-14), 45.4 (CH-20), 45.2 (CH₂), 42.4 (C-13), 40.4 (CH₂), 34.6 (CH₂), 34.2 (CH₂), 30.3 (CH₃-4'/5'), 29.8 (CH₃-4'/5'), 27.1 (CH₂), 25.9 (CH₃-^tBu), 23.0 (CH₂), 21.4 (CH₂), 18.1 (C-^tBu), 17.6 (CH₂), 14.2 (CH₃-18), 7.3 (CH₃-TES), 6.9 (CH₂-TES), -4.7 (CH₃-Si), -5.1 (CH₃-Si); **IR** (ATR, cm⁻¹): ν 3334, 2951, 2934, 2874, 2857, 1462, 1363, 1252, 1166, 1083, 1033, 1006, 974, 837, 774, 744; **MS** (ESI): *m/z* (%) 403.4 ([M - OH - TBSOH]⁺, 100), 271.4 ([M - OH - TBSOH - TESOH]⁺, 69); **HRMS** (ESI): *m/z* calculated for C₃₂H₆₄NaO₃Si₂ [M + Na]⁺ 575.4286, found 585.4291; **TLC** (SiO₂; 20% EtOAc/hexane): R_f = 0.59.

(8β)-(20R,22S,24R)-Des-A,B-8-[(*tert*-butyldimethyl)silyloxy]-22,24-cyclo-21-(3'-[(triethyl)silyloxy]-3'-methylbutyl)cholan-25-ol (8c), (8β)-(20R,22R,24S)-Des-A,B-8-[(*tert*-butyldimethyl)silyloxy]-22,24-cyclo-21-(3'-[(triethyl)silyloxy]-3'-methylbutyl)cholan-25-ol (8a), (8β)-(20S,22R,24S)-Des-A,B-8-[(*tert*-butyldimethyl)silyloxy]-22,24-cyclo-21-(3'-[(triethyl)silyloxy]-3'-methylbutyl)cholan-25-ol (8d) and (8β)-(20S,22S,24R)-Des-A,B-8-[(*tert*-butyldimethyl)silyloxy]-22,24-cyclo-21-(3'-[(triethyl)silyloxy]-3'-methylbutyl)cholan-25-ol (8b): To a solution of **7a/7b** (207 mg, 0.37 mmol, 1.0 equiv.) in anhydrous PhMe (5 mL) at -78 °C was added CH₂I₂ (previously purified with Al₂O₃ by pipette column chromatography, 150 μL, 1.87 mmol, 5.0 equiv.), Et₂Zn (1.0 M in hexane, 1.87 mL, 1.87 mmol, 5.0 equiv.) dropwise and the solution was stirred at rt for 48 h. The mixture reaction was quenched with sat. aq. NaHCO₃ solution (15 mL) and the layers were separated. The aqueous phase was extracted with CH₂Cl₂ (3 x 15 mL) and the combined organic extracts were dried over Na₂SO₄, filtered and concentrated *in vacuo*. The residue was chromatographed on silicagel using 5-7% EtOAc/hexane as eluent, affording the starting material **7a/7b** in the first fractions as a colorless oil (29 mg, 14%)/(17 mg, 8%), the product **8c/8d** in the intermediate fractions as a colorless oil (30 mg, 14%)/(13 mg, 6%) and the product **8a/8b** in the last fractions as colorless oil (150 mg, 71%)/(180 mg, 85%). Compound **8c**: **¹H-NMR** (400 MHz, CDCl₃): δ 4.00 (q, *J* = 2.9 Hz, 1H, H-8), 3.72 – 3.20 (m, 2H, CH₂-25), 1.94 – 1.72 (m, 3H), 1.69 – 1.62 (m, 1H), 1.58 – 1.31 (m, 13H), 1.29 – 1.21 (m, 3H), 1.19 (s, 6H, CH₃-4', CH₃-5'), 0.94 (t, *J* = 7.9 Hz, 9H, CH₃-TES), 0.88 (s, 9H, CH₃-^tBu), 0.85 (s, 3H, CH₃-18), 0.80 – 0.64 (m, 2H), 0.56 (q, *J* = 7.9 Hz, 6H, CH₂-TES), 0.50 – 0.40 (m, 2H, CH₂-23), 0.00 (s, 3H, CH₃-Si), -0.01 (s, 3H, CH₃-Si); **¹³C-NMR** (101 MHz, CDCl₃): δ 73.5 (C-3'), 69.6 (CH-8), 67.7 (CH₂-25), 54.6 (CH-17), 53.0 (CH-14), 46.2 (CH₂), 43.5 (CH-20), 42.4 (C-13), 40.2 (CH₂), 34.7 (CH₂), 34.0 (CH₂), 30.1 (CH₃-4'/5'), 29.9 (CH₃-4'/5'), 27.0 (CH₂), 26.0 (CH₃-^tBu), 23.0 (CH₂), 22.4 (CH-24), 19.6 (CH₂), 19.4 (CH-22), 18.2 (C-^tBu), 17.9 (CH₂), 14.0 (CH₃-18), 13.0 (CH₂-23), 7.3 (CH₃-TES), 7.0 (CH₂-TES), -4.6 (CH₃-Si), -5.0 (CH₃-Si); **IR** (ATR, cm⁻¹): ν 3363, 2952, 2928, 2873, 2856, 1462, 1378, 1251, 1166,

1083, 1032, 837, 774, 743, 724; **MS** (ESI): m/z (%) 589.5 ($[M + Na]^+$, 18), 435.4 ($[M - OTES]^+$, 21), 417.4 ($[M - OH - TESOH]^+$, 100), 285.3 ($[M - OH - TBSOH - TESOH]^+$, 42); **HRMS** (ESI): m/z calculated for $C_{33}H_{66}NaO_3Si_2$ $[M + Na]^+$ 589.4443, found 589.4450; **TLC** (SiO_2 ; 20% EtOAc/hexane): $R_f = 0.54$. Compound **8a**: **1H -NMR** (400 MHz, $CDCl_3$): δ 4.04 – 3.96 (m, 1H, H-8), 3.72 – 3.19 (m, 2H, CH_2 -25), 1.91 – 1.77 (m, 3H), 1.69 – 1.65 (m, 1H), 1.53 – 1.33 (m, 14H), 1.19 (s, 6H, CH_3 -4', CH_3 -5'), 0.94 (t, $J = 7.9$ Hz, 9H, CH_3 -TES), 0.88 (s, 9H, CH_3 - t Bu), 0.86 (s, 3H, CH_3 -18), 0.80 – 0.68 (m, 2H), 0.57 (q, $J = 7.9$ Hz, 6H, CH_2 -TES), 0.49 – 0.37 (m, 2H), 0.35 – 0.29 (m, 2H, CH_2 -23), 0.00 (s, 3H, CH_3 -Si), -0.01 (s, 3H, CH_3 -Si); **^{13}C -NMR** (101 MHz, $CDCl_3$): δ 73.5 (C-3'), 69.5 (CH-8), 67.4 (CH_2 -25), 54.4 (CH-17), 53.0 (CH-14), 46.1 (CH_2), 43.6 (CH-20), 42.4 (C-13), 40.3 (CH_2), 34.6 (CH_2), 33.8 (CH_2), 30.1 (CH_3 -4'/5'), 30.1 (CH_3 -4'/5'), 27.2 (CH_2), 25.9 (CH_3 - t Bu), 23.4 (CH-24), 23.1 (CH_2), 22.1 (CH-22), 19.5 (CH_2), 18.2 (C- t Bu), 17.9 (CH_2), 13.9 (CH_3 -18), 8.2 (CH_2 -23), 7.3 (CH_3 -TES), 7.3 (CH_2 -TES), -4.7 (CH_3 -Si), -5.0 (CH_3 -Si); **IR** (ATR, cm^{-1}): ν 3348, 2924, 2928, 2872, 2854, 1463, 1378, 1252, 1167, 1083, 1032, 837, 774, 743, 723; **MS** (ESI): m/z (%) 589.4 ($[M + Na]^+$, 12), 435.4 ($[M - OTES]^+$, 17), 417.4 ($[M - OH - TESOH]^+$, 82), 285.3 ($[M - OH - TBSOH - TESOH]^+$, 100); **HRMS** (ESI): m/z calculated for $C_{33}H_{66}NaO_3Si_2$ $[M + Na]^+$ 589.4443, found 589.4435; **TLC** (SiO_2 ; 20% EtOAc/hexane): $R_f = 0.52$. Compound **8d**: **1H -NMR** (400 MHz, $CDCl_3$): δ 4.02 – 3.99 (m, 1H, H-8), 3.66 – 3.25 (m, 2H, CH_2 -25), 1.83 – 1.65 (m, 4H), 1.42 – 1.23 (m, 18H), 1.19 (s, 3H, CH_3 -4'/5'), 1.19 (s, 3H, CH_3 -4'/5'), 0.97 – 0.92 (m, 12H, CH_3 -18, CH_3 -TES), 0.88 (s, 9H, CH_3 - t Bu), 0.56 (q, $J = 7.9$ Hz, 6H, CH_2 -TES), 0.51 – 0.45 (m, 2H, CH_2 -23), 0.00 (s, 3H, CH_3 -Si), -0.01 (s, 3H, CH_3 -Si); **^{13}C -NMR** (101 MHz, $CDCl_3$): δ 73.6 (C-3'), 69.5 (CH-8), 67.8 (CH_2 -25), 55.2 (CH-17), 53.0 (CH-14), 46.4 (CH_2), 42.0 (CH-20), 39.8 (CH_2), 34.8 (CH_2), 34.1 (CH_2), 30.1 (CH_3 -4'/5'), 30.0 (CH_3 -4'/5'), 29.8 (C-13), 26.4 (CH_2), 25.9 (CH_3 - t Bu), 22.9 (CH_2), 22.4 (CH-24), 21.0 (CH-22), 19.3 (CH_2), 18.2 (C- t Bu), 17.8 (CH_2), 14.5 (CH_3 -18), 14.3 (CH_2 -23), 7.3 (CH_3 -TES), 6.9 (CH_2 -TES), -4.6 (CH_3 -Si), -5.0 (CH_3 -Si); **IR** (ATR, cm^{-1}): ν 3735, 2953, 2931, 2875, 2856, 1653, 1559, 1458, 1275, 1260, 1166, 1084, 1032, 837, 765, 749, 725; **MS** (ESI): m/z (%) 589.4 ($[M + Na]^+$, 5), 435.4 ($[M - OTES]^+$, 16), 417.4 ($[M - OH - TESOH]^+$, 100), 403.3 ($[M - OH - OTES - Me]^+$, 25); **HRMS** (ESI): m/z calculated for $C_{33}H_{66}NaO_3Si_2$ $[M + Na]^+$ 589.4443, found 589.4435; **TLC** (SiO_2 ; 20% EtOAc/hexane): $R_f = 0.54$. Compound **8b**: **1H -NMR** (400 MHz, $CDCl_3$): δ 4.04 – 3.95 (m, 1H, H-8), 3.89 – 3.01 (m, 2H, CH_2 -25), 1.89 – 1.55 (m, 6H), 1.48 – 1.21 (m, 16H), 1.18 (s, 6H, CH_3 -4', CH_3 -5'), 0.94 (t, $J = 7.9$ Hz, 9H, CH_3 -TES), 0.90 (s, 3H, CH_3 -18), 0.88 (s, 9H, CH_3 - t Bu), 0.56 (q, $J = 7.9$ Hz, 6H, CH_2 -TES), 0.43 – 0.34 (m, 2H, CH_2 -23), 0.00 (s, 3H, CH_3 -Si), -0.01 (s, 3H, CH_3 -Si); **^{13}C -NMR** (101 MHz, $CDCl_3$): δ 73.6 (C-3'), 69.5 (CH-8), 67.4 (CH_2 -25), 55.3 (CH-17), 52.9 (CH-14), 46.0 (CH_2), 42.2 (C-13), 41.4 (CH-20), 39.7 (CH_2), 34.7 (CH_2), 33.6 (CH_2), 30.2 (CH_3 -4'/5'), 30.0 (CH_3 -4'/5'), 25.9 (CH_3 - t Bu), 25.6 (CH_2), 23.3 (CH-24), 22.9 (CH_2), 22.4 (CH-22), 20.4 (CH_2), 18.2 (C- t Bu), 17.7 (CH_2), 14.7 (CH_3 -18), 9.5 (CH_2 -24), 7.3 (CH_3 -TES), 6.9 (CH_2 -TES), -4.7 (CH_3 -Si), -5.0 (CH_3 -Si); **IR** (ATR, cm^{-1}): ν 3650, 2952, 2931, 2909, 2875, 2857, 1458, 1363, 1254, 1166, 1083, 1031, 837, 766, 746, 725; **MS** (ESI): m/z (%) 589.4 ($[M + Na]^+$, 46), 435.4 ($[M - OTES]^+$, 16), 417.4 ($[M - OH - TESOH]^+$, 49), 285.3 ($[M - OH - TBSOH - TESOH]^+$, 100); **HRMS** (ESI): m/z calculated for $C_{33}H_{66}NaO_3Si_2$ $[M + Na]^+$ 589.4443, found 589.4437; **TLC** (SiO_2 ; 20% EtOAc/hexane): $R_f = 0.52$.

(8 β)-(20R,22R,24S)-Des-A,B-8-[(*tert*-butyldimethyl)silyloxy]-22,24-cyclo-21-(3'-[(triethyl)silyloxy]-3'-methylbutyl)cholan-25-al (9a) and (8 β)-(20S,22S,24R)-Des-A,B-8-[(*tert*-butyldimethyl)silyloxy]-22,24-cyclo-21-(3'-[(triethyl)silyloxy]-3'-methylbutyl)cholan-25-al (9b): To a solution of **8a/8b** (37 mg, 0.065 mmol, 1.0 equiv.)

in dry CH₂Cl₂ (1.0 mL) at rt was added MS (4Å, 33 mg, 500 mg/mmol of **8a/8b**), NMO (23 mg, 0.20 mmol, 3.0 equiv.), TPAP (3.5 mg, 10 μmol, 15 mol%) and the solution was stirred at this temperature for 1.5 h. The solvent was removed *in vacuo* and the residue was chromatographed on silicagel using 0.6% EtOAc/hexane as eluent, affording the product as a colorless oil (34 mg, 95%)/(33 mg, 92%). Compound **9a**: ¹H-NMR (400 MHz, CDCl₃): δ 8.94 (d, *J* = 5.8 Hz, 1H, CHO), 4.01 – 3.97 (m, 1H, H-8), 1.89 – 1.65 (m, 5H), 1.55 – 1.31 (m, 14H), 1.26 – 1.22 (m, 2H), 1.20 (s, 6H, CH₃-4', CH₃-5'), 1.18 – 1.15 (m, 2H, CH₂-23), 0.94 (t, *J* = 7.9 Hz, 9H, CH₃-TES), 0.87 (s, 9H, CH₃-^tBu), 0.86 (s, 3H CH₃-18), 0.56 (q, *J* = 7.7 Hz, 6H, CH₂-TES), 0.00 (s, 3H, CH₃-Si), -0.02 (s, 3H, CH₃-Si); ¹³C-NMR (101 MHz, CDCl₃): δ 201.4 (CHO), 73.4 (C-3'), 69.4 (CH-8), 54.2 (CH-17), 52.9 (CH-14), 45.9 (CH₂), 43.0 (CH-20), 42.5 (C-13), 40.3 (CH₂), 34.5 (CH₂), 34.0 (CH₂), 33.0 (CH-24), 30.1 (CH₃-4'/5'), 30.0 (CH₃-4'/5'), 27.4 (CH-22), 27.2 (CH₂), 25.9 (CH₃-^tBu), 23.0 (CH₂), 19.7 (CH₂), 18.2 (C-^tBu), 17.9 (CH₂), 14.0 (CH₃-18), 12.8 (CH₂-23), 7.3 (CH₃-TES), 6.9 (CH₂-TES), -4.7 (CH₃-Si), -5.0 (CH₃-Si); IR (ATR, cm⁻¹): ν 2956, 2924, 2872, 2854, 1715, 1463, 1378, 1251, 1166, 1085, 1033, 837, 774, 743; MS (ESI): *m/z* (%) 587.4 ([M + Na]⁺, 11), 565.4 ([M + H]⁺, 14), 433.4 ([M - OTES]⁺, 100); HRMS (ESI): *m/z* calculated for C₃₃H₆₄NaO₄Si₂ [M + Na]⁺ 587.4486, found 587.4278; TLC (SiO₂; 10% EtOAc/hexane): R_f = 0.65. Compound **9b**: ¹H-NMR (400 MHz, CDCl₃): δ 8.97 (d, *J* = 5.6 Hz, 1H, CHO), 4.02 – 3.96 (m, 1H, H-8), 1.81 – 1.62 (m, 5H), 1.62 – 1.21 (m, 18H), 1.19 (s, 6H, CH₃-4', CH₃-5'), 1.05 – 0.98 (m, 2H, CH₂-23), 0.94 (t, *J* = 7.9 Hz, 9H, CH₃-TES), 0.90 (s, 3H CH₃-18), 0.87 (s, 9H, CH₃-^tBu), 0.56 (q, *J* = 7.1 Hz, 6H, CH₂-TES), 0.00 (s, 3H, CH₃-Si), -0.02 (s, 3H, CH₃-Si); ¹³C-NMR (101 MHz, CDCl₃): δ 201.7 (CHO), 73.4 (C-3'), 69.4 (CH-8), 55.0 (CH-17), 52.8 (CH-14), 46.0 (CH₂), 42.2 (C-13), 41.1 (CH-20), 39.8 (CH₂), 34.6 (CH₂), 33.9 (CH₂), 32.9 (CH-24), 30.2 (CH₃-4'/5'), 30.0 (CH₃-4'/5'), 27.7 (CH-22), 25.9 (CH₃-^tBu), 25.5 (CH₂), 22.8 (CH₂), 20.1 (CH₂), 18.1 (C-^tBu), 17.6 (CH₂), 14.8 (CH₃-18), 14.6 (CH₂-23), 7.3 (CH₃-TES), 6.9 (CH₂-TES), -4.7 (CH₃-Si), -5.0 (CH₃-Si); IR (ATR, cm⁻¹): ν 2954, 2927, 2875, 2855, 1696, 1462, 1379, 1363, 1252, 1232, 1165, 1084, 1033, 837, 774, 744, 724; MS (ESI): *m/z* (%) 587.4 ([M + Na]⁺, 4), 563.4 ([M - H]⁺, 45), 433.4 ([M - OTES]⁺, 100); HRMS (ESI): *m/z* calculated for C₃₃H₆₃O₃Si₂ [M - OH]⁺ 563.4310, found 563.4323; TLC (SiO₂; 10% EtOAc/hexane): R_f = 0.65.

Ethyl (25E)-(8β)-(20R,22S,24R)-des-A,B-8-[(tert-butyl)dimethylsilyloxy]-22,24-cyclo-27-nor-21-(3'-[(triethyl)silyloxy]-3'-methylbutyl)cholestan-25-en-26-carboxyl ester (10a) and Ethyl (25E)-(8β)-(20S,22R,24S)-des-A,B-8-[(tert-butyl)dimethylsilyloxy]-22,24-cyclo-27-nor-21-(3'-[(triethyl)silyloxy]-3'-methylbutyl)cholestan-25-en-26-carboxyl ester (10b): To a solution of **9a/9b** (125 mg, 0.22 mmol, 1.0 equiv.) in anhydrous THF (3 mL) at rt was added triphenylcarbethoxymethylenephosphorane (306 mg, 0.88 mmol, 4.0 equiv.) and the solution was stirred at this temperature for 38 h. Then the solvent was removed *in vacuo* and the residue was chromatographed on silicagel using 0.2% EtOAc/hexane as eluent, affording the product as a colorless oil (131 mg, 99%)/(131 mg, 99%). Compound **10a**: ¹H-NMR (400 MHz, CDCl₃): 6.43 (dd, *J* = 15.4, 10.2 Hz, 1H, H-25), 5.82 (d, *J* = 15.4 Hz, 1H, H-26), 4.16 (q, *J* = 7.1 Hz, 2H, CH₂-OEt), 3.99 (q, *J* = 2.8 Hz, 1H, H-8), 2.33 – 2.20 (m, 1H), 1.92 – 1.62 (m, 5H), 1.53 – 1.33 (m, 13H), 1.30 – 1.25 (m, 5H), 1.19 (s, 6H, CH₃-4', CH₃-5'), 0.94 (t, *J* = 7.9 Hz, 9H, CH₃-TES), 0.88 (s, 9H, CH₃-^tBu), 0.85 (s, 3H, CH₃-18), 0.82 – 0.74 (m, 2H, CH₂-23), 0.56 (q, *J* = 8.0 Hz, 6H, CH₂-TES), 0.00 (s, 3H, CH₃-Si), -0.01 (s, 3H, CH₃-Si); ¹³C-NMR (101 MHz, CDCl₃): δ 167.1 (C=O), 154.0 (CH-25), 117.7 (CH-26), 73.5 (C-3'), 69.5 (CH-8), 60.1 (CH₂-OEt), 54.4 (CH-17), 53.0 (CH-14), 46.0 (CH₂), 43.9 (CH-20), 42.4 (C-13), 40.2 (CH₂), 34.6 (CH₂), 33.8 (CH₂),

30.1 (CH₃-4'/5'), 30.1 (CH₃-4'/5'), 28.6 (CH-22), 27.4 (CH₂), 26.0 (CH₃-^tBu), 24.7 (CH-24), 23.1 (CH₂), 19.5 (CH₂), 18.2 (C-^tBu), 17.9 (CH₂), 14.5 (CH₃-18), 14.1 (CH₂-23), 13.9 (CH₃-OEt), 7.3 (CH₃-TES), 6.9 (CH₂-TES), -4.6 (CH₃-Si), -5.0 (CH₃-Si); **IR** (ATR, cm⁻¹): ν 2954, 2926, 2874, 2854, 1720, 1645, 1462, 1378, 1364, 1261, 1167, 1143, 1033, 837, 774, 743, 723; **MS** (ESI): *m/z* (%) 657.5 ([M + Na]⁺, 9), 635.5 ([M + H]⁺, 13), 503.4 ([M - OTES]⁺, 20), 371.3 ([M + H - TBSOH - TESOH]⁺, 100); **HRMS** (ESI): *m/z* calculated for C₃₇H₇₀NaO₄Si₂ [M + Na]⁺ 657.4705, found 657.4689; **TLC** (SiO₂; 10% EtOAc/hexane): R_f = 0.70. Compound **10b**: **¹H-NMR** (400 MHz, CDCl₃): 6.43 (dd, *J* = 15.4, 10.2 Hz, 1H, H-25), 5.82 (dd, *J* = 15.4 Hz, 1H, H-26), 4.16 (q, *J* = 7.1 Hz, 2H, CH₂-OEt), 4.05 – 3.95 (m, 1H, H-8), 1.95 – 1.84 (m, 1H), 1.80 – 1.61 (m, 4H), 1.59 – 1.48 (m, 1H), 1.46 – 1.30 (m, 11H), 1.30 – 1.21 (m, 7H), 1.19 (s, 6H, CH₃-4', CH₃-5'), 0.94 (t, *J* = 7.9 Hz, 9H, CH₃-TES), 0.88 (s, 12H, CH₃-^tBu, CH₃-18), 0.85 – 0.76 (m, 2H, CH₂-23), 0.56 (q, *J* = 7.9 Hz, 6H, CH₂-TES), 0.00 (s, 3H, CH₃-Si), -0.02 (s, 3H, CH₃-Si); **¹³C-NMR** (101 MHz, CDCl₃): δ 167.0 (C=O), 154.3 (CH-25), 117.8 (CH-26), 73.5 (C-3'), 69.5 (CH-8), 60.1 (CH₂-OEt), 55.0 (CH-17), 52.9 (CH-14), 46.0 (CH₂), 42.1 (C-13), 42.0 (CH-20), 39.6 (CH₂), 34.7 (CH₂), 33.8 (CH₂), 30.1 (CH₃-4'/5'), 30.1 (CH₃-4'/5'), 28.1 (CH-22), 25.9 (CH₃-^tBu), 25.0 (CH-24), 22.8 (CH₂), 19.9 (CH₂), 18.2 (C-^tBu), 17.6 (CH₂), 15.4 (CH₂-23), 14.6 (CH₃-18), 14.4 (CH₃-OEt), 7.3 (CH₃-TES), 6.9 (CH₂-TES), -4.6 (CH₃-Si), -5.0 (CH₃-Si); **IR** (ATR, cm⁻¹): ν 2954, 2925, 2874, 2854, 1720, 1645, 1463, 1378, 1364, 1261, 1166, 1143, 1034, 837, 772, 746, 723; **MS** (ESI): *m/z* (%) 657.5 ([M + Na]⁺, 25), 635.5 ([M + H]⁺, 28), 503.4 ([M - OTES]⁺, 28), 371.3 ([M + H - TBSOH - TESOH]⁺, 100); **HRMS** (ESI): *m/z* calculated for C₃₇H₇₀NaO₄Si₂ [M + Na]⁺ 657.4705, found 657.4709; **TLC** (SiO₂; 10% EtOAc/hexane): R_f = 0.70.

Ethyl (8β)-(20R,22S,24R)-des-A,B-8-[(*tert*-butyldimethyl)silyloxy]-22,24-cyclo-27-nor-21-(3'-[(triethyl)silyloxy]-3'-methylbutyl)cholestane-26-carboxyl ester (11a) and Ethyl (8β)-(20S,22R,24S)-des-A,B-8-[(*tert*-butyldimethyl)silyloxy]-22,24-cyclo-27-nor-21-(3'-[(triethyl)silyloxy]-3'-methylbutyl)cholestane-26-carboxyl ester (11b): To a solution of [(PPh₃)CuH]₆ (64 mg, 0.033 mmol, 15 mol%) in anhydrous PhMe (1.0 mL) at rt was added PHMS (60 μL, 0.33 mmol, 1.5 equiv.) dropwise, a solution of **10a/10b** (140 mg, 0.22 mmol, 1.0 equiv.) in anhydrous PhMe (2.5 mL) and the resulting red mixture was stirred at this temperature for 3 days. The mixture was diluted with Et₂O (10 mL) and washed with sat. aq. NH₄Cl solution (10 mL), sat. aq. NaHCO₃ solution (2 x 10 mL) and sat. aq. NaCl solution (2 x 10 mL). The organic phase was dried over Na₂SO₄, filtered and concentrated *in vacuo*. The residue was chromatographed on silicagel using 0.1% EtOAc/hexane as eluent, affording the product as a colorless oil (130 mg, 93%)/(133 mg, 95%). Compound **11a**: **¹H-NMR** (400 MHz, CDCl₃): 4.14 – 4.09 (m, 2H, CH₂-OEt), 4.03 – 3.97 (m, 1H, H-8), 2.36 (t, *J* = 7.7 Hz, 2H, CH₂-26), 2.03 – 1.94 (m, 1H), 1.90 – 1.76 (m, 3H), 1.67 (d, *J* = 11.5 Hz, 1H), 1.59 – 1.30 (m, 15H), 1.25 (t, *J* = 7.1 Hz, 6H), 1.18 (s, 6H, CH₃-4', CH₃-5'), 0.94 (t, *J* = 7.9 Hz, 9H, CH₃-TES), 0.88 (s, 9H, CH₃-^tBu), 0.84 (s, 3H, CH₃-18), 0.59 – 0.52 (m, 8H, CH₂-23, CH₂-TES), 0.00 (s, 3H, CH₃-Si), -0.01 (s, 3H, CH₃-Si); **¹³C-NMR** (101 MHz, CDCl₃): δ 174.0 (C=O), 73.6 (C-3'), 69.6 (CH-8), 60.3 (CH₂-OEt), 54.5 (CH-17), 53.1 (CH-14), 46.1 (CH₂), 43.9 (CH-20), 42.4 (C-13), 40.3 (CH₂), 34.7 (CH₂), 34.3 (CH₂), 33.7 (CH₂), 30.1 (CH₃-4'/5'), 30.1 (CH₃-4'/5'), 29.8 (CH₂), 27.1 (CH₂), 26.0 (CH₃-^tBu), 24.2 (CH-24), 23.2 (CH₂), 20.5 (CH-22), 19.6 (CH₂), 18.2 (C-^tBu), 17.9 (CH₂), 14.4 (CH₃-18), 13.9 (CH₃-OEt), 9.7 (CH₂-23), 7.3 (CH₃-TES), 7.0 (CH₂-TES), -4.6 (CH₃-Si), -5.0 (CH₃-Si); **IR** (ATR, cm⁻¹): ν 2954, 2930, 2907, 2875, 1739, 1645, 1438, 1377, 1364, 1259, 1166, 1113, 1028, 804, 737, 723, 690; **MS** (ESI): *m/z* (%) 659.5 ([M + Na]⁺, 4), 505.4 ([M - OTES]⁺, 47), 373.3 ([M + H - TBSOH - TESOH]⁺, 100); **HRMS** (ESI): *m/z* calculated for C₃₇H₇₃O₄Si₂ [M

+ H]⁺ 637.5042, found 637.5041; **TLC** (SiO₂; 5% EtOAc/hexane): R_f = 0.38. Compound **11b**: **¹H-NMR** (400 MHz, CDCl₃): 4.12 (q, *J* = 7.1 Hz, 2H, CH₂-OEt), 4.02 – 3.98 (m, 1H, H-8), 2.35 (t, *J* = 7.6 Hz, 2H, CH₂-26), 2.03 – 1.90 (m, 2H), 1.84 – 1.75 (m, 1H), 1.72 – 1.62 (m, 3H), 1.62 – 1.45 (m, 2H), 1.45 – 1.29 (m, 12H), 1.25 (t, *J* = 7.1 Hz, 6H), 1.18 (s, 6H, CH₃-4', CH₃-5'), 0.94 (t, *J* = 7.9 Hz, 9H, CH₃-TES), 0.88 (s, 12H, CH₃-^tBu, CH₃-18), 0.63 – 0.49 (m, 8H, CH₂-23, CH₂-TES), 0.01 (s, 3H, CH₃-Si), -0.01 (s, 3H, CH₃-Si); **¹³C-NMR** (101 MHz, CDCl₃): δ 174.0 (C=O), 73.6 (C-3'), 69.5 (CH-8), 60.3 (CH₂-OEt), 55.3 (CH-17), 53.0 (CH-14), 46.1 (CH₂), 42.1 (C-13), 41.8 (CH-20), 39.6 (CH₂), 34.8 (CH₂), 34.5 (CH₂), 33.5 (CH₂), 30.2 (CH₃-4'/5'), 30.0 (CH₃-4'/5'), 29.9 (CH₂), 26.0 (CH₃-^tBu), 25.6 (CH₂), 24.3 (CH-24), 23.0 (CH₂), 20.5 (CH₂), 20.3 (CH-22), 18.2 (C-^tBu), 17.7 (CH₂), 14.7 (CH₃-18), 14.4 (CH₃-OEt), 10.9 (CH₂-23), 7.3 (CH₃-TES), 6.9 (CH₂-TES), -4.6 (CH₃-Si), -5.0 (CH₃-Si); **IR** (ATR, cm⁻¹): ν 2953, 2927, 2875, 2856, 1740, 1645, 1463, 1377, 1364, 1252, 1168, 1083, 1030, 837, 774, 742, 723; **MS** (ESI): *m/z* (%) 659.5 ([M + Na]⁺, 4), 505.4 ([M - OTES]⁺, 57), 373.3 ([M + H - TBSOH - TESOH]⁺, 100); **HRMS** (ESI): *m/z* calculated for C₃₇H₇₃O₄Si₂ [M + H]⁺ 637.5042, found 637.4919; **TLC** (SiO₂; 5% EtOAc/hexane): R_f = 0.38.

(8β)-(20R,22S,24S)-des-A,B-8-[(*tert*-butyldimethyl)silyloxy]-22,24-cyclo-24-dihomo-21-(3'-[(triethyl)silyloxy]-3'-methylbutyl)cholestan-27-ol (12a) and (8β)-(20S,22S,24R)-des-A,B-8-[(*tert*-butyldimethyl)silyloxy]-22,24-cyclo-24-dihomo-21-(3'-[(triethyl)silyloxy]-3'-methylbutyl)cholestan-27-ol (12b): To a solution of **11a/11b** (162 mg, 0.26 mmol, 1.0 equiv.) in anhydrous THF (2.5 mL) at -78 °C was added MeLi (1.6 M in Et₂O, 0.8 mL, 1.28 mmol, 5.0 equiv.) dropwise and the solution was stirred at this temperature for 16 h. The mixture reaction was quenched by addition of H₂O (3 mL) and the layers were separated. The aqueous phase was extracted with EtOAc (3 x 4 mL) and the combined organic extracts were dried over Na₂SO₄, filtered and concentrated *in vacuo*. The residue was chromatographed on silicagel using 2-5% EtOAc/hexane as eluent, affording the ketone **16a/16b** in the first fractions as a colorless oil (19 mg, 12%)/(27 mg/17%) and the alcohol **12a/12b** in the last fractions as a colorless oil (139 mg, 81%)/(142 mg, 83%). Compound **12a**: **¹H-NMR** (400 MHz, CDCl₃): 4.01 (m, 1H, H-8), 1.99 – 1.60 (m, 7H), 1.58 – 1.22 (m, 22H), 1.19 (s, 12H, CH₃-4', CH₃-5', CH₃-28, CH₃-29), 0.95 (t, *J* = 7.6 Hz, 9H, CH₃-TES), 0.88 (s, 9H, CH₃-^tBu), 0.85 (s, 3H, CH₃-18), 0.70 – 0.64 (m, 1H), 0.60 – 0.49 (m, 8H, CH₂-23, CH₂-TES), 0.31 – 0.26 (m, 1H), 0.20 – 0.14 (m, 1H), 0.00 (s, 3H, CH₃-Si), -0.01 (s, 3H, CH₃-Si); **¹³C-NMR** (101 MHz, CDCl₃): δ 73.6 (C-3'), 71.0 (C-27), 69.7 (CH-8), 54.5 (CH-17), 53.1 (CH-14), 46.2 (CH₂), 44.0 (CH-20), 42.4 (C-13), 40.3 (CH₂), 34.7 (CH₂), 33.7 (CH₂), 30.1 (CH₃-4'/5'), 30.0 (CH₃-4'/5'), 29.4 (CH₃-28/29), 29.3 (CH₃-28/29), 29.1 (CH₂), 27.2 (CH₂), 26.0 (CH₃-^tBu), 24.4 (CH-24), 23.2 (CH₂), 21.4 (CH-22), 19.6 (CH₂), 18.2 (C-^tBu), 17.9 (CH₂), 13.9 (CH₃-18), 9.8 (CH₂-23), 7.3 (CH₃-TES), 7.0 (CH₂-TES), -4.6 (CH₃-Si), -5.0 (CH₃-Si); **IR** (ATR, cm⁻¹): ν 3378, 2954, 2929, 2874, 2857, 1462, 1378, 1363, 1254, 1166, 1082, 1031, 837, 774, 743, 722; **MS** (ESI): *m/z* (%) 645.5 ([M + Na]⁺, 3), 491.4 ([M - OTES]⁺, 50), 359.3 ([M + H - TBSOH - TESOH]⁺, 100), 341.3 ([M - OH - TBSOH - TESOH]⁺, 27); **HRMS** (ESI): *m/z* calculated for C₃₇H₇₅O₃Si₂ [M + H]⁺ 623.5249, found 623.5239; **TLC** (SiO₂; 20% EtOAc/hexane): R_f = 0.57. Compound **12b**: **¹H-NMR** (400 MHz, CDCl₃): 4.03 – 3.97 (m, 1H, H-8), 2.01 – 1.95 (m, 1H), 1.82 – 1.76 (m, 1H), 1.75 – 1.61 (m, 4H), 1.60 – 1.46 (m, 5H), 1.43 – 1.28 (m, 13H), 1.18 (s, 6H, CH₃-4'/28, CH₃-5'/29), 1.18 (s, 6H, CH₃-4'/28, CH₃-5'/29), 0.94 (t, *J* = 7.9 Hz, 9H, CH₃-TES), 0.89 (s, 3H, CH₃-18), 0.88 (s, 9H, CH₃-^tBu), 0.55 (q, *J* = 7.9 Hz, 6H, CH₂-TES), 0.51 – 0.36 (m, 2H, CH₂-23), 0.30 – 0.21 (m, 1H), 0.17 – 0.06 (m, 1H), 0.00 (s, 3H, CH₃-Si), -0.01 (s, 3H, CH₃-Si); **¹³C-NMR** (101 MHz, CDCl₃): δ 73.6 (C-3'), 71.1 (C-27), 69.5 (CH-8), 55.2 (CH-17), 53.0 (CH-14), 46.2

(CH₂), 43.5 (CH₂), 42.1 (C-13), 41.9 (CH-20), 39.6 (CH₂), 34.8 (CH₂), 33.4 (CH₂), 30.2 (CH₃-4'/5'), 30.0 (CH₃-4'/5'), 29.3 (CH₃-28/29), 29.3 (CH₃-28/29), 29.1 (CH₂), 25.9 (CH₃-^tBu), 25.7 (CH₂), 24.2 (CH-24), 23.0 (CH₂), 21.0 (CH-22), 20.5 (CH₂), 18.2 (C-^tBu), 17.7 (CH₂), 14.7 (CH₃-18), 10.8 (CH₂-23), 7.3 (CH₃-TES), 6.9 (CH₂-TES), -4.7 (CH₃-Si), -5.0 (CH₃-Si); **IR** (ATR, cm⁻¹): ν 3375, 2956, 2922, 2853, 1463, 1378, 1365, 1252, 1165, 1083, 1032, 888, 837, 745, 722; **MS** (ESI): m/z (%) 645.5 ([M + Na]⁺, 37), 491.4 ([M - OTES]⁺, 44), 359.3 ([M + H - TBSOH - TESOH]⁺, 100), 341.3 ([M - OH - TBSOH - TESOH]⁺, 28); **HRMS** (ESI): m/z calculated for C₃₇H₇₄NaO₃Si₂ [M + Na]⁺ 645.5069, found 645.5077; **TLC** (SiO₂; 20% EtOAc/hexane): R_f = 0.57.

(8 β)-(20R,22S,24S)-des-A,B-22,24-cyclo-24-dihomo-21-(3'-hydroxy-3'-methylbutyl)cholestan-8,27-diol (13a) and (8 β)-(20S,22R,24R)-des-A,B-22,24-cyclo-24-dihomo-21-(3'-hydroxy-3'-methylbutyl)cholestan-8,27-diol (13b): To a solution of **12a/12b** (74 mg, 0.12 mmol, 1.0 equiv.) in anhydrous THF (2.5 mL) at rt was added TBAF (1.0 M in THF, 1.2 mL, 1.20 mmol, 10.0 equiv.) and the solution was stirred at this temperature for 5 days. The solvent was removed *in vacuo* and the residue was chromatographed on silicagel using 35% EtOAc/hexane as eluent, affording the product as a white solid (43 mg, 94%)/(44 mg, 96%). Compound **13a**: **¹H-NMR** (400 MHz, CDCl₃): 4.10 – 4.06 (m, 1H, H-8), 1.97 – 1.87 (m, 2H), 1.84 – 1.76 (m, 2H), 1.75 – 1.69 (m, 1H), 1.63 – 1.29 (m, 20H), 1.21 (s, 6H, CH₃-4'/28, CH₃-5'/29), 1.19 (s, 3H, CH₃-4'/28, CH₃-5'/29), 1.19 (s, 3H, CH₃-26/27/4'/5'), 0.87 (s, 3H, CH₃-18), 0.72 – 0.64 (m, 1H), 0.58 – 0.46 (m, 1H), 0.32 – 0.25 (m, 1H), 0.21 – 0.07 (m, 2H); **¹³C-NMR** (101 MHz, CDCl₃): δ 71.3 (C-3'), 71.0 (C-27), 69.5 (CH-8), 54.3 (CH-17), 52.6 (CH-14), 44.9 (CH₂), 43.9 (CH-20), 42.3 (CH₂), 42.1 (C-13), 39.9 (CH₂), 33.7 (CH₂), 33.6 (CH₂), 29.5 (CH₃-4'/5'), 29.5 (CH₃-4'/5'), 29.3 (CH₃-28/29), 29.3 (CH₃-28/29), 29.0 (CH₂), 27.1 (CH₂), 24.2 (CH-24), 22.6 (CH₂), 21.3 (CH-22), 19.4 (CH₂), 17.7 (CH₂), 13.7 (CH₃-18), 9.8 (CH₂-23); **IR** (ATR, cm⁻¹): ν 3402, 2959, 2926, 2872, 2855, 1463, 1483, 1376, 1363, 1261, 1170, 1114, 1028, 737, 723, 691; **MS** (ESI): m/z (%) 417.3 ([M + Na]⁺, 17), 395.4 ([M + H]⁺, 72), 377.3 ([M - OH]⁺, 100), 359.3 ([M - H₂O - OH]⁺, 37), 341.3 ([M - 2H₂O - OH]⁺, 10); **HRMS** (ESI): m/z calculated for C₂₅H₄₆NaO₃ [M + Na]⁺ 417.3339, found 417.3340; **TLC** (SiO₂; 50% EtOAc/hexane): R_f = 0.25. Compound **13b**: **¹H-NMR** (400 MHz, CDCl₃): 4.10 – 4.06 (m, 1H, H-8), 2.07 – 2.00 (m, 1H), 1.87 – 1.66 (m, 5H), 1.60 – 1.29 (m, 20H), 1.20 (s, 6H, CH₃-4'/28, CH₃-5'/29), 1.18 (s, 6H, CH₃-4'/28, CH₃-5'/29), 0.91 (s, 3H, CH₃-18), 0.54 – 0.39 (m, 2H, CH₂-23), 0.33 – 0.08 (m, 2H); **¹³C-NMR** (101 MHz, CDCl₃): δ 71.3 (C-3'), 71.0 (C-27), 69.5 (CH-8), 55.0 (CH-17), 52.5 (CH-14), 44.9 (CH₂), 43.4 (CH₂), 41.8 (C-13), 41.7 (CH-20), 39.3 (CH₂), 33.8 (CH₂), 33.4 (CH₂), 29.5 (CH₃-4'/5'), 29.4 (CH₃-4'/5'), 29.3 (CH₃-28/29), 29.3 (CH₃-28/29), 29.0 (CH₂), 25.7 (CH₂), 24.0 (CH-24), 22.4 (CH₂), 21.1 (CH-22), 20.3 (CH₂), 17.4 (CH₂), 14.5 (CH₃-18), 10.7 (CH₂-23); **IR** (ATR, cm⁻¹): ν 3387, 2958, 2925, 2854, 1462, 1377, 1244, 1146, 1060, 941, 909, 888; **MS** (ESI): m/z (%) 417.3 ([M + Na]⁺, 100), 395.4 ([M + H]⁺, 10), 377.3 ([M - OH]⁺, 79), 359.3 ([M - H₂O - OH]⁺, 71), 341.3 ([M - 2H₂O - OH]⁺, 51); **HRMS** (ESI): m/z calculated for C₂₅H₄₆NaO₃ [M + Na]⁺ 417.3339, found 417.3348; **TLC** (SiO₂; 50% EtOAc/hexane): R_f = 0.25.

(20R,22S,24S)-des-A,B-22,24-cyclo-24-dihomo-27-hydroxy-21-[3'-hydroxy-21-(3'-hydroxy-3'-methylbutyl)cholestan-8-one (14a) and (20S,22R,24R)-des-A,B-22,24-cyclo-24-dihomo-27-hydroxy-21-[3'-hydroxy-21-(3'-[(trimethylsilyloxy]-3'-methylbutyl)cholestan-8-one (14b): To a solution of **13a/13b** (42 mg, 0.11 mmol, 1.0 equiv.) in dry CH₂Cl₂ (2.5 mL) at rt was added PDC (120 mg, 0.32 mmol, 3.0 equiv.) and the solution was stirred at this temperature for 4 h. The solvent was removed *in vacuo*

and the residue was chromatographed on silicagel using 40% EtOAc/hexane as eluent, affording the product as a colorless oil (39 mg, 95%)/(37 mg, 91%). Compound **14a**: **¹H-NMR** (400 MHz, CDCl₃): 2.50 – 2.43 (m, 1H), 2.30 – 2.20 (m, 2H), 2.03 – 1.83 (m, 5H), 1.74 – 1.39 (m, 15H), 1.22 (s, 6H, CH₃-4'/28, CH₃-5'/29), 1.18 (s, 6H, CH₃-4'/28, CH₃-5'/29), 0.82 – 0.65 (m, 2H), 0.56 (s, 3H, CH₃-18), 0.54 – 0.48 (m, 1H), 0.34 – 0.29 (m, 1H), 0.21 – 0.10 (m, 2H); **¹³C-NMR** (101 MHz, CDCl₃): δ 212.3 (C=O), 71.2 (C-3'), 71.0 (C-27), 61.9 (CH-17), 54.4 (CH-14), 50.1 (C-13), 44.8 (CH₂), 44.0 (CH-20), 43.2 (CH₂), 41.1 (CH₂), 38.5 (CH₂), 33.8 (CH₂), 29.4 (CH₃-4'/5'), 29.4 (CH₃-4'/5'), 29.4 (CH₃-28/29), 29.3 (CH₃-28/29), 28.9 (CH₂), 27.3 (CH₂), 24.2 (CH₂), 24.0 (CH-24), 21.4 (CH-22), 19.4 (CH₂), 19.1 (CH₂), 12.7 (CH₃-18), 9.9 (CH₂-23); **IR** (ATR, cm⁻¹): ν 3404, 2963, 2931, 2875, 1707, 1466, 1456, 1378, 1364, 1266, 1215, 1179, 1152, 943, 903, 766; **MS** (ESI): *m/z* (%) 415.3 ([M + Na]⁺, 11), 393.3 ([M + H]⁺, 33), 375.3 ([M - OH]⁺, 100), 357.3 ([M - H₂O - OH]⁺, 69); **HRMS** (ESI): *m/z* calculated for C₂₅H₄₄NaO₃ [M + Na]⁺ 415.3183, found 415.3183; **TLC** (SiO₂; 70% EtOAc/hexane): R_f = 0.42. Compound **14b**: **¹H-NMR** (400 MHz, CDCl₃): 2.47 – 2.41 (m, 1H), 2.27 – 2.19 (m, 2H), 2.04 – 1.67 (m, 7H), 1.57 – 1.32 (m, 13H), 1.19 (s, 6H, CH₃-4'/28, CH₃-5'/29), 1.17 (s, 3H, CH₃-4'/5'/28/29), 1.17 (s, 3H, CH₃-4'/5'/28/29), 0.90 – 0.81 (m, 2H), 0.60 (s, 3H, CH₃-18), 0.52 – 0.42 (m, 2H, CH₂-23), 0.29 – 0.14 (m, 2H); **¹³C-NMR** (101 MHz, CDCl₃): δ 212.5 (C=O), 71.1 (C-3'), 70.8 (C-27), 61.9 (CH-17), 54.9 (CH-14), 50.0 (C-13), 44.8 (CH₂), 43.3 (CH₂), 42.5 (CH-20), 41.1 (CH₂), 37.9 (CH₂), 33.4 (CH₂), 29.5 (CH₃-4'/5'), 29.4 (CH₃-4'/5'), 29.3 (CH₃-28/29), 29.3 (CH₃-28/29), 28.8 (CH₂), 26.1 (CH₂), 24.0 (CH₂), 23.8 (CH-24), 21.2 (CH-22), 20.1 (CH₂), 19.0 (CH₂), 13.4 (CH₃-18), 10.7 (CH₂-23); **IR** (ATR, cm⁻¹): ν 3404, 2958, 2926, 2874, 2854, 1769, 1759, 1464, 1378, 1244, 1215, 1167, 1055, 837, 774, 721; **MS** (ESI): *m/z* (%) 415.3 ([M + Na]⁺, 14), 393.3 ([M + H]⁺, 64), 375.3 ([M - OH]⁺, 100), 357.3 ([M - H₂O - OH]⁺, 66); **HRMS** (ESI): *m/z* calculated for C₂₅H₄₄NaO₃ [M + Na]⁺ 415.3183, found 415.3173; **TLC** (SiO₂; 70% EtOAc/hexane): R_f = 0.42.

(20R,22S,24S)-des-A,B-22,24-cyclo-24-dihomo-27-[(trimethyl)silyloxy]-21-(3'-[(trimethyl)silyloxy]-3'-methylbutyl)cholestan-8-one (3a) and (20R,22R,24R)-des-A,B-22,24-cyclo-24-dihomo-27-[(trimethyl)silyloxy]-21-(3'-[(trimethyl)silyloxy]-3'-methylbutyl)cholestan-8-one (3b): To a solution of **14a/14b** (39 mg, 0.099 mmol, 1.0 equiv.) in anhydrous THF (2.5 mL) at rt was added TMS-Im (120 mg, 1.98 mmol, 20.0 equiv.) and the solution was stirred at this temperature for 40 h. The mixture was diluted with hexane (5 mL) and washed with H₂O (3 x 5 mL). The organic phase was dried over Na₂SO₄, filtered and concentrated *in vacuo* to give the product as a colorless oil (50 mg, 95%)/(50 mg, 95%), which was used in the next step without any further purification due to it was spectroscopically pure. Compound **3a**: **¹H-NMR** (400 MHz, CDCl₃): 2.47 (dd, *J* = 11.4, 7.5 Hz, 1H, H-14), 2.31 – 2.21 (m, 2H), 2.05 – 1.83 (m, 5H), 1.77 – 1.63 (m, 3H), 1.59 – 1.36 (m, 12H), 1.22 (s, 6H, CH₃-4'/28, CH₃-5'/29), 1.18 (s, 6H, CH₃-4'/28, CH₃-5'/29), 0.84 – 0.65 (m, 2H), 0.58 (s, 3H, CH₃-18), 0.52 – 0.43 (m, 1H), 0.34 – 0.29 (m, 1H), 0.21 – 0.12 (m, 2H), 0.11 (s, 9H, CH₃-Si), 0.09 (s, 9H, CH₃-Si); **¹³C-NMR** (101 MHz, CDCl₃): δ 212.4 (C=O), 74.2 (C-3'), 74.0 (C-27), 62.0 (CH-17), 54.5 (CH-14), 50.1 (C-13), 45.8 (CH₂), 44.2 (CH-20), 44.2 (CH₂), 41.2 (CH₂), 38.6 (CH₂), 33.8 (CH₂), 30.1 (CH₃-4'/5'), 30.0 (CH₃-4'/5'), 30.0 (CH₃-28, CH₃-29), 29.1 (CH₂), 27.4 (CH₂), 24.3 (CH₂), 24.1 (CH-24), 21.4 (CH-22), 19.5 (CH₂), 19.1 (CH₂), 12.7 (CH₃-18), 10.0 (CH₂-23), 2.8 (CH₃-Si), 2.8 (CH₃-Si); **IR** (ATR, cm⁻¹): ν 2959, 2923, 2872, 2853, 1719, 1463, 1379, 1364, 1248, 1166, 1153, 1046, 837, 752; **MS** (ESI): *m/z* (%) 559.4 ([M + Na]⁺, 6), 537.4 ([M + H]⁺, 25), 357.3 ([M + H - 2TMSOH]⁺, 100); **HRMS** (ESI): *m/z* calculated for C₃₁H₆₁O₃Si₂ [M + H]⁺ 537.4154, found 537.4164; **TLC** (SiO₂; 10% EtOAc/hexane):

$R_f = 0.47$. Compound **3b**: $^1\text{H-NMR}$ (400 MHz, CDCl_3): 2.46 (dd, $J = 11.0, 7.6$ Hz, 1H, H-14), 2.30 – 2.21 (m, 3H), 2.05 – 1.71 (m, 7H), 1.56 – 1.48 (m, 4H), 1.40 – 1.33 (m, 6H), 1.20 (s, 6H, $\text{CH}_3\text{-4}'/28, \text{CH}_3\text{-5}'/29$), 1.19 (s, 3H, $\text{CH}_3\text{-4}'/5'/28/29$), 1.17 (s, 3H, $\text{CH}_3\text{-4}'/5'/28/29$), 0.85 – 0.79 (m, 2H), 0.62 (s, 3H, $\text{CH}_3\text{-18}$), 0.51 – 0.42 (m, 2H), 0.31 – 0.13 (m, 2H), 0.10 (s, 9H, $\text{CH}_3\text{-Si}$), 0.09 (s, 9H, $\text{CH}_3\text{-Si}$); $^{13}\text{C-NMR}$ (101 MHz, CDCl_3): δ 212.5 (C=O), 74.2 (C-3'), 73.9 (C-27), 62.1 (CH-17), 55.1 (CH-14), 50.0 (C-13), 45.7 (CH₂), 44.3 (CH₂), 42.7 (CH-20), 41.2 (CH₂), 38.0 (CH₂), 33.5 (CH₂), 30.4 (CH₃-4'/5'), 30.1 (CH₃-4'/5'), 30.1 (CH₃-28/29), 29.7 (CH₃-28/29), 29.0 (CH₂), 26.3 (CH₂), 24.1 (CH₂), 23.8 (CH-24), 21.4 (CH-22), 20.2 (CH₂), 19.0 (CH₂), 13.4 (CH₃-18), 10.7 (CH₂-23), 2.8 (CH₃-Si), 2.8 (CH₃-Si); **IR** (ATR, cm^{-1}): ν 2958, 2924, 2854, 1709, 1464, 1378, 1364, 1248, 1215, 1153, 1043, 839; **MS** (ESI): m/z (%) 537.4 ($[\text{M} + \text{H}]^+$, 3), 375.3 ($[\text{M} + \text{H} - \text{TMS} - \text{OTMS}]^+$, 100), 357.3 ($[\text{M} + \text{H} - 2\text{TMSOH}]^+$, 89); **HRMS** (ESI): m/z calculated for $\text{C}_{31}\text{H}_{61}\text{O}_3\text{Si}_2$ $[\text{M} + \text{H}]^+$ 537.4154, found 537.4169; **TLC** (SiO_2 ; 10% EtOAc/hexane): $R_f = 0.47$.

(20R,22S,24S)-1,3-Bis[O-(tert-butyl dimethyl)silyl]-22,24-cyclo-24-dihomo-27-(O-(trimethyl)silyl)-21-(3'-[(trimethyl)silyloxy]-3'-methylbutyl)calcitriol (17a)
(20S,22R,24R)-1,3-Bis[O-(tert-butyl dimethyl)silyl]-22,24-cyclo-24-dihomo-27-(O-(trimethyl)silyl)-21-(3'-[(trimethyl)silyloxy]-3'-methylbutyl)calcitriol (17b): To a solution of the phosphine oxide **4** (170 mg, 0.29 mmol, 7.0 equiv.) in anhydrous THF (2.0 mL) at -78 °C was added *n*-BuLi (2.5 M in hexane, 98 μL , 0.25 mmol, 6.0 equiv.) dropwise and the red solution was stirred at this temperature for 2 h. Then, was added **3a/3b** (22 mg, 0.041 mmol, 1.0 equiv.) in anhydrous THF (0.5 mL) and the resulting mixture was stirred at this temperature in the absence of light for 16 h. The mixture reaction was quenched with sat. aq. NH_4Cl solution (4 mL) and the layers were separated. The aqueous phase was extracted with EtOAc (3 x 5 mL) and the combined organic extracts were dried over Na_2SO_4 , filtered and concentrated *in vacuo*. The residue was chromatographed on silicagel using 0.6% EtOAc/hexane as eluent, affording the product as a colorless oil (34 mg, 94%)/(34 mg, 94%). Compound **16a**: $^1\text{H-NMR}$ (400 MHz, CDCl_3): 6.24, 6.03 (2 d, $J_{AB} = 11.2$ Hz, 2H, H-6, H-7), 5.29 (d, $^2J = 1.4$ Hz, 1H, Z-H-19), 4.97 (d, $^2J = 1.4$ Hz, 1H, E-H-19), 4.37 (dd, $J = 6.5, 3.6$ Hz, 1H, H-1), 4.18 (dq, $J = 7.2, 3.6$ Hz, 1H, H-3), 2.90 – 2.76 (m, 1H), 2.44 (dd, $J = 13.1, 3.4$ Hz, 1H, H-14), 2.22 (dd, $J = 13.2, 7.3$ Hz, 1H), 2.05 – 1.61 (m, 9H), 1.56 – 1.31 (m, 14H), 1.21 (s, 6H, $\text{CH}_3\text{-4}'/28, \text{CH}_3\text{-5}'/29$), 1.18 (s, 6H, $\text{CH}_3\text{-4}'/28, \text{CH}_3\text{-5}'/29$), 0.87 (s, 18H, $\text{CH}_3\text{-}^t\text{Bu}$), 0.67 (t, $J = 9.6$ Hz, 1H), 0.47 (s, 3H, $\text{CH}_3\text{-18}$), 0.39 – 0.11 (m, 3H, CH₂-23), 0.11 (s, 9H, $\text{CH}_3\text{-Si}$), 0.10 (s, 9H, $\text{CH}_3\text{-Si}$), 0.07 (s, 3H, $\text{CH}_3\text{-Si}$), 0.06 (s, 6H, $\text{CH}_3\text{-Si}$), 0.06 (s, 3H, $\text{CH}_3\text{-Si}$); $^{13}\text{C-NMR}$ (101 MHz, CDCl_3): δ 148.4 (C-8), 141.3 (C-5), 135.1 (C-10), 123.3 (CH-6), 118.0 (CH-7), 111.3 (CH₂-19), 74.3 (C-3'), 74.0 (C-27), 72.1 (CH-1), 67.7 (CH-3), 56.3 (CH-17), 54.4 (CH-14), 46.1 (CH₂), 46.0 (C-13), 45.8 (CH₂), 44.9 (CH₂), 44.7 (CH-20), 44.2 (CH₂), 40.2 (CH₂), 33.9 (CH₂), 30.1 (CH₃-4'/5'), 30.0 (CH₃-4'/5'), 30.0 (CH₃-28/29), 30.0 (CH₃-28/29), 29.2 (CH₂), 29.1 (CH₂), 27.4 (CH₂), 26.0 (CH₃-^tBu), 26.0 (CH₃-^tBu), 24.3 (CH-24), 23.7 (CH₂), 22.2 (CH₂), 21.5 (CH-22), 19.6 (CH₂), 18.4 (C-^tBu), 18.3 (C-^tBu), 12.2 (CH₃-18), 9.8 (CH₂-23), 2.8 (CH₃-Si), -4.5 (CH₃-Si), -4.5 (CH₃-Si), -4.6 (CH₃-Si), -4.9 (CH₃-Si); **IR** (ATR, cm^{-1}): ν 2955, 2926, 2855, 1471, 1458, 1379, 1363, 1249, 1166, 1084, 1047, 837, 755; **MS** (ESI): m/z (%) 923.7 ($[\text{M} + \text{Na}]^+$, 3), 901.7 ($[\text{M} + \text{H}]^+$, 13), 739.6 ($[\text{M} + \text{H} - \text{OTMS} - \text{TMS}]^+$, 60), 607.5 ($[\text{M} - \text{OTBS} - \text{OTMS} - \text{TMS}]^+$, 100); **HRMS** (ESI): m/z calculated for $\text{C}_{52}\text{H}_{100}\text{NaO}_4\text{Si}_4$ $[\text{M} + \text{Na}]^+$ 923.6591, found 923.6606; **TLC** (SiO_2 ; 10% EtOAc/hexane): $R_f = 0.82$. Compound **16b**: $^1\text{H-NMR}$ (400 MHz, CDCl_3): 6.25, 6.03 (2 d, $J_{AB} = 11.2$ Hz, 2H, H-6, H-7), 5.18 (d, $^2J = 2.3$ Hz, 1H, Z-H-19), 4.87 (d, $^2J = 2.3$ Hz, 1H, E-H-19), 4.37 (dd, $J = 6.6, 3.6$ Hz, 1H, H-1), 4.19 (dq, $J = 7.2,$

3.6 Hz, 1H, H-3), 2.90 – 2.76 (m, 1H), 2.45 (dd, $J = 13.2, 3.4$ Hz, 1H, H-14), 2.22 (dd, $J = 13.2, 7.3$ Hz, 1H), 2.11 – 1.93 (m, 2H), 1.89 – 1.61 (m, 8H), 1.54 – 1.45 (m, 5H), 1.43 – 1.22 (m, 13H), 1.20 (s, 6H, CH₃-4'/28, CH₃-5'/29), 1.18 (s, 3H, CH₃-4'/5'/28/29'), 1.16 (s, 3H, CH₃-4'/5'/28/29'), 0.87 (s, 18H, CH₃-^tBu), 0.51 (s, 3H, CH₃-18), 0.47 – 0.38 (m, 1H), 0.28 – 0.12 (m, 2H, CH₂-23), 0.11 (s, 9H, CH₃-Si), 0.11 (s, 9H, CH₃-Si), 0.09 (s, 3H, CH₃-Si), 0.06 (s, 6H, CH₃-Si), 0.06 (s, 3H, CH₃-Si); ¹³C-NMR (101 MHz, CDCl₃): δ 148.4 (C-8), 141.5 (C-5), 135.0 (C-10), 123.4 (CH-6), 117.9 (CH-7), 111.3 (CH₂-19), 74.3 (C-3'), 73.9 (C-27), 72.2 (CH-1), 67.7 (CH-3), 56.4 (CH-17), 54.9 (CH-14), 46.1 (CH₂), 45.8 (C-13), 45.8 (CH₂), 44.9 (CH₂), 44.3 (CH₂), 43.0 (CH-20), 39.5 (CH₂), 33.6 (CH₂), 30.4 (CH₃-4'/5'), 30.1 (CH₃-4'/5'), 30.1 (CH₃-28/29), 29.8 (CH₃-28/29), 29.1 (CH₂), 26.2 (CH₂), 26.0 (CH₃-^tBu), 26.0 (CH₃-^tBu), 24.0 (CH-24), 23.4 (CH₂), 22.1 (CH₂), 21.2 (CH-22), 20.5 (CH₂), 18.4 (C-^tBu), 18.3 (C-^tBu), 13.0 (CH₃-18), 10.8 (CH₂-23), 2.8 (CH₃-Si), -4.5 (CH₃-Si), -4.5 (CH₃-Si), -4.6 (CH₃-Si), -4.9 (CH₃-Si); IR (ATR, cm⁻¹): ν 2955, 2926, 2854, 1651, 1461, 1379, 1363, 1251, 1086, 1046, 836, 763, 751; MS (ESI): m/z (%) 923.7 ([M + Na]⁺, 8), 901.7 ([M + H]⁺, 32), 739.6 ([M + H – OTMS – TMS]⁺, 64), 607.5 ([M – OTBS – OTMS – TMS]⁺, 100); HRMS (ESI): m/z calculated for C₅₂H₁₀₀NaO₄Si₄ [M + Na]⁺ 923.6591, found 923.6601; TLC (SiO₂; 10% EtOAc/hexane): R_f = 0.83.

(20R,22S,24S)-22,24-Cyclo-24-dihomo-21-(3'-hydroxy-3'-methylbutyl)calcitriol (UG-481) and (20S,22R,24R)-22,24-Cyclo-24-dihomo-21-(3'-hydroxy-3'-methylbutyl)calcitriol (UG-480): To a solution of **17a/17b** (15 mg, 0.017 mmol, 1.0 equiv.) in anhydrous THF (1.0 mL) at rt was added TBAF (1.0 M in THF, 200 μL, 0.20 mmol, 12.0 equiv.) and the solution was stirred at this temperature in the absence of light for 22 h. The solvent was removed *in vacuo* and the residue was chromatographed on silicagel using EtOAc as eluent, affording the product as a colorless oil (9 mg, 99%)/(9 mg, 99%). Compound **UG-481**: ¹H-NMR (400 MHz, CDCl₃): 6.38, 6.03 (2 d, $J_{AB} = 11.2$ Hz, 2H, H-6, H-7), 5.32 (br s, 1H, Z-H-19), 5.00 (br s, 1H, E-H-19), 4.43 (dd, $J = 7.8, 4.2$ Hz, 1H, H-1), 4.22 (dq $J = 6.6, 3.3$ Hz, 1H, H-3), 3.30 (br, 1H, OH), 2.83 (dd, $J = 12.2, 4.1$, 1H), 2.59 (dd, $J = 13.6, 3.7$ Hz, 1H, H-14), 2.31 (dd, $J = 13.5, 6.5$ Hz, 1H), 2.05 – 1.98 (m, 3H), 1.94 – 1.89 (m, 3H), 1.72 – 1.67 (m, 5H), 1.57 – 1.50 (m, 16H), 1.22 (s, 6H, CH₃-4'/28, CH₃-5'/29), 1.19 (s, 3H, CH₃-4'/5'/28/29), 1.19 (s, 3H, CH₃-4'/5'/28/29), 0.70 – 0.64 (m, 1H), 0.48 (s, 3H, CH₃-18), 0.32 (ddt, $J = 14.2, 9.5, 4.4$ Hz, 1H), 0.20 – 0.10 (m, 2H, CH₂-23); ¹³C-NMR (101 MHz, CDCl₃): δ 147.8 (C-8), 143.3 (C-5), 133.1 (C-10), 125.1 (CH-6), 117.2 (CH-7), 111.9 (CH₂-19), 71.3 (C-3'), 71.1 (C-27), 70.9 (CH-1), 67.0 (CH-3), 56.2 (CH-17), 54.2 (CH-14), 46.1 (C-13), 45.4 (CH₂), 44.9 (CH₂), 44.5 (CH-20), 43.3 (CH₂), 43.0 (CH₂), 40.0 (CH₂), 33.9 (CH₂), 29.5 (CH₃-4'/5'), 29.5 (CH₃-4'/5'), 29.3 (CH₃-28, CH₃-29), 29.2 (CH₂), 29.0 (CH₂), 27.2 (CH₂), 24.2 (CH-24), 24.2 (CH₂), 23.3 (CH₂), 21.5 (CH-22), 19.5 (CH₂), 12.3 (CH₃-18), 9.8 (CH₂-23); IR (ATR, cm⁻¹): ν 3358, 3200, 3182, 2955, 2924, 2854, 1660, 1633, 1466, 1412, 1377, 1276, 1261, 1195, 1063, 763, 750; MS (ESI): 551.4 ([M + Na]⁺, 24), 529.4 ([M + H]⁺, 83), 511.4 ([M – OH]⁺, 60), 493.4 ([M – H₂O – OH]⁺, 100); HRMS (ESI): m/z calculated for C₃₄H₅₇O₄ [M + H]⁺ 529.4251, found 529.4252; TLC (SiO₂; EtOAc): R_f = 0.24. Compound **UG-480**: ¹H-NMR (400 MHz, CDCl₃): 6.24, 6.03 (2 d, $J_{AB} = 11.2$ Hz, 2H, H-6, H-7), 5.33 (br s, 1H, Z-H-19), 5.00 (br s, 1H, E-H-19), 4.43 (dd, $J = 7.5, 4.2$ Hz, 1H, H-1), 4.18 (dq, $J = 6.4, 3.3$ Hz, 1H, H-3), 2.84 (dd, $J = 12.1, 3.6$ Hz, 1H), 2.60 (dd, $J = 13.2, 3.0$ Hz, 1H, H-14), 2.32 (dd, $J = 13.4, 6.4$ Hz, 1H), 2.07 – 1.89 (m, 6H), 1.74 – 1.62 (m, 10H), 1.57 – 1.49 (m, 6H), 1.45 – 1.33 (m, 8H), 1.25 (s, 3H, CH₃-4'/5'/28/29), 1.12 (s, 3H, CH₃-4'/5'/28/29), 1.19 (s, 3H, CH₃-4'/5'/28/29), 1.19 (s, 3H, CH₃-4'/5'/28/29), 0.52 (s, 3H, CH₃-18), 0.29 – 0.13 (m, 3H, CH₂-23); ¹³C-NMR (101 MHz, CDCl₃): δ 147.8 (C-8),

143.5 (C-5), 132.9 (C-10), 125.2 (CH-6), 117.1 (CH-7), 111.9 (CH₂-19), 71.3 (C-3'), 71.0 (C-27), 70.9 (CH-1), 67.0 (CH-3), 56.3 (CH-17), 54.8 (CH-14), 45.9 (C-13), 45.4 (CH₂), 45.0 (CH₂), 43.4 (CH₂), 43.0 (CH₂), 42.8 (CH-20), 39.4 (CH₂), 33.5 (CH₂), 29.5 (CH₃-4'/5'), 29.5 (CH₃-4'/5'), 29.4 (CH₃-28/29), 29.3 (CH₃-28/29), 29.3 (CH₂), 28.9 (CH₂), 26.1 (CH₂), 24.1 (CH-24), 23.5 (CH₂), 22.2 (CH₂), 21.1 (CH-22), 20.4 (CH₂), 13.3 (CH₃-18), 10.8 (CH₂-23); **IR** (ATR, cm⁻¹): ν 3378, 2957, 2924, 2853, 1667, 1463, 1378, 1362, 1273, 1257, 1212, 1149, 1056, 954, 911, 751; **MS** (ESI): 551.4 ([M + Na]⁺, 10), 529.4 ([M + H]⁺, 53), 511.4 ([M - OH]⁺, 38), 493.4 ([M - H₂O - OH]⁺, 24), 202.2 (100); **HRMS** (ESI): *m/z* calculated for C₃₄H₅₇O₄ [M + H]⁺ 529.4251, found 529.4256; **TLC** (SiO₂; EtOAc): R_f = 0.28.

Proliferation. The human breast carcinoma (MCF-7) cell line was obtained from the American Tissue Culture Company (Rockville, MD). Cells were seeded in 96-well plates (10,000 cells/well) in DMEM medium, supplemented with 10% fetal bovine serum, 2 mM glutamax, 100 U/mL penicillin, and 100 μ g/mL streptomycin (all from Fisher Scientific). The following day, cells were incubated for 72 h with increasing concentrations of 1,25(OH)₂D₃, **UG-480** or **UG-481**. Thereafter, 1 μ Ci [methyl-³H]thymidine (ICN Biomedicals, Costa Mesa, CA) was added to the cultures and cells were semi-automatically harvested on filterplates after an additional 4 h of incubation (GF/C Filter and Filtermate Universal Harvester, Packard Instrument, Meriden, CT). Counting was performed using a microplate scintillation counter (Topcount, Packard).

Biochemistry, crystallization and structure determination. The cDNA encoding His-tagged zVDR LBD (156-453) was cloned into pET28b. The recombinant proteins were produced in Escherichia coli BL21 DE3, grown ON at 18 °C after induction with 1 mM IPTG (OD600 of ~0.7). Soluble proteins were purified on Ni Hitrap FFcrude column (Cytiva), followed by His tag removal by thrombin cleavage and by size exclusion chromatography on HiLoad Superdex 75 column (Cytiva) equilibrated in Tris 20 mM pH7, NaCl 200 mM, TCEP 1 mM. The proteins were concentrated to 3-7 mg/mL with an Amicon Ultra 30 kDa MWCO. The concentrated protein was incubated with a 2-fold excess of ligand and a 3-fold excess of the NCoA1 coactivator peptide (RHKILHRLQLQEGSPS). The crystallization experiments were carried out by hanging drop vapor diffusion at 290 K by mixing equal volume (1 μ L) of protein-ligand complex and of reservoir solution (Li₂SO₄ 1.8 M). The crystals of the complex were transferred to artificial mother liquor containing Li₂SO₄ 2.2 M and flash cooled in liquid nitrogen. X-ray data were collected on the Proxima2 beamline at Soleil synchrotron. The raw data were processed with XDS²⁴ and scaled with AIMLESS.²⁵ The structures were solved and refined using Buster²⁶ and Phenix²⁷ and iterative model building using COOT.²⁸ Crystallographic refinement statistics are presented in Supplementary Table 7.

Molecular docking simulations were performed using as structural template the VDR/calcitriol complex deposited in the Protein Databank under the code 1DB1.⁸ VDR structure was extracted from the complex, with waters and calcitriol being removed prior to docking assays. Affinity grids were constructed using Autogrid4, considering a cubic box of 22 x 22 x 22 Å positioned at the center of mass of the crystallographic ligand (i.e. calcitriol). Grids were constructed using three biased interaction points based on current knowledge with respect to calcitriol pharmacophoric contacts (Figure S4). Docking runs were performed using AutoDock-GPU,²⁹ while the AutoDock Bias methodology was used to favor pharmacophoric biases in the docking affinity grids.³⁰

Molecular dynamics simulations were carried out using the Amber22 software package.³¹ Simulations were obtained using the pmemd.cuda code, with computations being performed in CUDA compatible GPU cards. Initial structures intended for MD simulations were obtained from the lowest energy structure resulting from docking assays, after which an explicit solvent TIP3P water box was constructed around the solute, assuring a minimum distance of 10 Å between the solute and the boundary of the box. The simulation protocol included energy minimization and heating stages, after which an equilibration phase (10 ns) was performed prior to obtaining the production trajectory (100 ns). The system was simulated at a constant temperature of 300 °K, using a timestep of 2 fs. Restraints (1 kcal mol⁻¹ Å⁻²) were applied on the protein backbone to maintain the tertiary structure of VDR during the simulation of the ligand interaction. The SHAKE algorithm was applied to constrain all bonds involving hydrogen atoms. Simulations were performed using computational resources from CCAD - Universidad Nacional de Córdoba (<https://ccad.unc.edu.ar>), which are part of SNCAD - MinCyT, República Argentina.

Structural analyses on the simulated trajectories were performed using the CPPTRAJ and MDAnalysis packages.^{32,33} Three dimensional visualizations were generated using VMD v.1.9,³⁴ while 2D interaction maps were obtained using LigPlot + v.2.2.³⁵

ASSOCIATED CONTENT

Supporting Information. Additional supplemental figures and tables, synthetic procedures, and purity HPLC traces and characterization data for compounds can be found in SI appendix.

Molecular formula strings (CSV) with biochemical source data (CSV).

Homology models and tables for the FEP calculations.

Accession Codes. Atomic coordinates for the X-ray structures of zVDR LBD/**UG-480** (PDB 9EYR) and zVDR LBD/**UG-481** (PDB 9FBF) are available from the RCSB Protein Data Bank.

AUTHOR INFORMATION

(YF) +34 986812323, e-mail: yagamare@uvigo.es

(MAQ) +54 351 5353850 int 55437, e-mail: alfredoq@fcq.unc.edu.ar

(NR) +33.369.48.52.93, e-mail: rochel@igbmc.fr

ACKNOWLEDGEMENTS

This work was supported financially by the Xunta de Galicia (ED431C2017/70). The work of the NMR, MS, IR and DRX divisions of the research support services of the University of Vigo (C.A.C.T.I.) is also gratefully acknowledged. U.G.B. is grateful to Xunta de Galicia for predoctoral fellowship. We thank A. McEwen for help in X-ray data collection, and the staff of PX2 beam line of SOLEIL synchrotron for assistance during X-ray data collection. The research was also supported by French Infrastructure for Integrated Structural Biology (FRISBI) [ANR-10-INBS-05]; Instruct-ERIC; Agence Nationale de la Recherche under the program Investissements d'Avenir [ANR-10-LABX-0030-INRT, ANR-10-IDEX-0002-02]. Evaluation of the biological activity was financially supported by Fonds voor Wetenschappelijk Onderzoek-Vlaanderen (FWO grant GOD0120N). Mario Alfredo Quevedo would like to acknowledge the Centro de Computación de Alto Desempeño (CCAD-UNC, Córdoba, Argentina) for granting access to supercomputing resources.

ABBREVIATIONS USED

1,25(OH)₂D₃, 1 α ,25-dihydroxyvitaminD₃; ELE, electrostatic; LBD, ligand binding domain; LBP, ligand binding pocket; MD, molecular dynamics; VDR, vitamin D receptor; VDW, van der Waals

References

1. Eelen, G.; Verlinden, L.; De Clercq, P.; Vandevallé, M.; Bouillon, R.; Verstuyf, A. Vitamin D analogs and coactivators. *Anticancer Res.* **2006**, *26*, 2717-2721.
2. Posner, G.H.; Kahraman, M. Organic chemistry of vitamin D analogues (deltanoids). *Eur. J. Org. Chem.* **2003**, 3889-3895.
3. Ferronato, M.J.; Obiol, D.J.; Alonso, E.N.; Guevara, J.A.; Grioli, S.M.; Mascaró, M.; Rivadulla, M.L.; Martínez, A.; Gómez, G.; Fall, Y.; et al. Synthesis of a novel analog of calcitriol and its biological evaluation as antitumor agent. *J. Steroid Biochem. Mol. Biol.* **2019**, *185*, 118-136.
4. Ferronato, M.J.; Alonso, E.N.; Salomón, D.G.; Fermento, M.E.; Gandini, N.A.; Quevedo, M.A.; Mascaró, E.; Vitale, C.; Fall, Y.; Facchinetti, M.M.; et al. Antitumoral effects of the alkynylphosphonate analogue of calcitriol EM1 on glioblastoma multiforme cells. *J. Steroid Biochem. Mol. Biol.* **2018**, *178*, 22-35.
5. Ferronato, M.J.; Alonso, E.N.; Gandini, N.A.; Fermento, M.E.; Villegas, M.E.; Quevedo, M.A.; Arevalo, J.; Romero, A.L.; Rivadulla, M.L.; Gómez, G.; et al. The UVB1 vitamin D analogue inhibits colorectal carcinoma progression. *J. Steroid Biochem. Mol. Biol.* **2016**, *163*, 193-205.
6. Obiol, D.J.; Martínez, A.; Ferronato, M.J.; Quevedo, M.A.; Grioli, S.M.; Alonso, E.N.; Gómez, G.; Fall, Y.; Facchinetti, M.M.; Curino, A.C. Novel calcitriol analogue with an oxolane group: In vitro, in vivo, and in silico studies. *Archiv der Pharmazie* **2019**, *352*, 1800315.
7. Ribone, S.R.; Ferronato, M.J.; Vitale, C.; Fall, Y.; Curino, A.C.; Facchinetti, M.M.; Quevedo, M.A. Vitamin D receptor exhibits different pharmacodynamic features in tumoral and normal microenvironments: A molecular modeling study. *J. Steroid Biochem. Mol. Biol.* **2020**, *200*, 105649.
8. Rochel, N.; Wurtz, J.M.; Mitschler, A.; Klaholz, B.; Moras, D. The crystal structure of the nuclear receptor for vitamin d bound to its natural ligand. *Mol. Cell* **2000**, *5*, 173-179.
9. Pazos, G.; Rivadulla, M.L.; Pérez-García, X.; Gándara, Z.; Pérez, M. Gemini Analogs of Vitamin D. *Curr. Top. Med. Chem.*, **2014**, *14*, 2388-2397.
10. Norman, A.W.; Manchand, P.S.; Uskokovic, M.R.; Okamura, W.H.; Takeuchi, J.A.; Bishop, J.E.; Hisatake, J.I.; Koeffler, H.P.; Peleg, S. Characterization of a Novel Analogue of 1 α , 25(OH)₂-vitamin D₃ with two side chains: Interaction with Its Nuclear Receptor and Cellular Actions. *J. Med. Chem.*, **2000**, *43*, 2719-2729.
11. Weyts, F.A.; Dhawan, P.; Zhang, X.; Bishop, J.E.; Uskokovic, M.R.; Jid, Y.; Studzinski, G.P.; Norman, A.W.; Christakos, S. Novel Gemini analogs of 1 α ,25-dihydroxyvitamin D₃ with enhanced transcriptional activity. *Biochem. Pharm.* **2004**, *67*, 1327-1336.
12. Maehr, H.; Uskokovic, M.R. Formal desymmetrization of the Diastereotopic Chains in Gemini Calcitriol Derivatives with two different Side Chains at C-20. *Eur. J. Org. Chem.* **2004**, 1703-1713.
13. Fall, Y.; Gómez, G.; Pérez, M.; Gándara, Z.; Pérez, X.; Pazos, G.; Kurz, G. Gemini Vitamin D₃ analogues, Synthetic Procedure and Applications. Spanish Patent Code P201000421, PCT/ES2011/000094, **2011**.

14. Ferronato, M.J.; Salomón, D.G.; Ferment, M.E.; Gandini, N.A.; Romero, A.L.; Rivadulla, M.L.; Pérez-García, X.; Gómez, G.; Pérez, M.; Fall, Y.; Facchinetti, M.M.; Curino, A.C. Vitamin D Analogue: Potent Antiproliferative Effects on Cancer Cell lines and Lack of Hypercalcemic activity. *Arch. Pharm.*, **2015**, *345*, 315-329
15. Santalla, H.; Garrido, F.; Gómez, G.; Fall, Y. A more reliable synthesis of a Gemini vitamin D analog, a potentially effective chemotherapeutic agent for the treatment of colorectal carcinomas. *Org. Chem. Front.* **2018**, *5*, 2016-2019.
16. Ferronato, M.J.; Serrano, M.N.; Lahuerta, E.J.A.; Morales, C.B.; Paolillo, G.; Aliguer, A.M.S.; Santalla, H.; Mascaró, M.; Vitale, C.; Fall, Y.; Arribas, J.; Facchinetti, M.M.; Curino, A.C. Vitamin D analogues exhibit antineoplastic activity in breast cancer patient-derived xenograft cells. *J. Steroid Biochem. Mol. Biol.* **2021**, *208*, 105735.
17. Belorusova, A.Y.; Rovito, D.; Chebaro, Y.; Doms, S.; Verlinden, L.; Verstuyf, A.; Metzger, D.; Rochel, N.; Laverny, G. Vitamin D Analogs Bearing C-20 Modifications Stabilize the Agonistic Conformation of Non-Responsive Vitamin D Receptor Variants. *Int J Mol Sci.* **2022**, *23*, 8445.
18. Pazos, G.; Pérez, M.; Gándara, Z.; Gómez, G.; Fall, Y. [3,3]-Sigmatropic rearrangement mediated synthesis of chiral building blocks for the preparation of Gemini and its analogs. *RSC Adv.*, **2016**, *6*, 61073-61076.
19. Lipshutz, B. H.; Servesko, J. M.; Taft, B. R. Asymmetric 1,4-hydrosilylations of α,β -unsaturated esters. *J. Am. Chem. Soc.* **2004**, *126*, 8352-8353.
20. Huet, T.; Maehr, H.; Lee, H.J.; Uskokovic, M.R.; Suh, N.; Moras, D.; Rochel, N. Structure-function study of Gemini derivatives with two different side chains at C-20, Gemini-0072 and Gemini-0097. *Medchemcomm.* **2011**, *2*, 424-429.
21. Maehr, H.; Rochel, N.; Lee, H.J.; Suh, N.; Uskokovic, M.R. Diastereotopic and deuterium effects in Gemini. *J Med Chem.* **2013**, *56*, 3878-3888.
22. Ciesielski, F.; Rochel, N.; Moras, D. Adaptability of the Vitamin D nuclear receptor to the synthetic ligand Gemini: remodelling the LBP with one side chain rotation. *J Steroid Biochem Mol Biol.* **2007**, *103*, 235-242.
23. Belorusova, A.Y.; Suh, N.; Lee, H.J.; So, J.Y.; Maehr, H.; Rochel, N. Structural analysis and biological activities of BXL0124, a Gemini analog of vitamin D. *J Steroid Biochem Mol Biol.* **2017**, *173*, 69-74.
24. Kabsch, W. Software XDS for image rotation, recognition and crystal symmetry assignment. *Acta Crystallogr., Sect. D: Biol. Crystallogr.* **2010**, *66*, 125-132.
25. Evans, P. Scaling and assessment of data quality. *Acta Crystallogr. Sect. D: Biol. Crystallogr.* **2006**, *62*, 72-82.
26. Smart, O.S.; Womack, T.O.; Flensburg, C.; Keller, P.; Paciorek, W.; Sharff, A.; Vornrhein, C.; Bricogne, G. Exploiting structure similarity in refinement: automated NCS and target-structure restraints in BUSTER. *Acta Crystallogr D Biol Crystallogr.* **2012**, *68*, 368-380.
27. Adams, P.D., Afonine, P.V., Bunkoczi, G., Chen, V.B., Davis, I.W., Echols, N., Headd, J.J., Hung, L.W., Kapral, G.J., Grosse-Kunstleve, R.W., et al. PHENIX: a comprehensive Python-based system for macromolecular structure solution. *Acta Crystallogr D Biol Crystallogr.* **2010**, *66*, 213-221.
28. Emsley, P.; Lohkamp, B.; Scott, W.G.; Cowtan, K. Features and development of Coot. *Acta Crystallogr D Biol Crystallog.* **2010**, *66*, 486-501.
29. Santos-Martins, D.; Solis-Vasquez, L.; Tillack, A.F.; Sanner, M.F.; Koch, A.; Forli, S. Accelerating autodock4 with gpus and gradient-based local search. *J Chem Theory Comput.* **2021**, *17*, 1060-1073.
30. Arcon, J.P.; Modenutti, C.P.; Avendaño, D.; Lopez, E.D.; Defelipe, L.A.; Ambrosio, F.A.; Turjanski, A.G.; Forli, S.; Marti, M.A. Autodock bias: improving binding mode

prediction and virtual screening using known protein-ligand interactions. *Bioinformatics* **2019**, *35*, 3836-3838.

31. Case, D.; Aktulga, H.; Belfon, K.; Ben-Shalom, I.; Berryman, J.; Brozell, S.; Cerutti, D.; Cheatham III, T.; Cisneros, G.; Cruzeiro, V. et al. Amber22, **2023**.

32. Roe, D.R.; Cheatham III, T.E. Ptraaj and cpptraj: software for processing and analysis of molecular dynamics trajectory data. *J Chem Theory Comput.* **2013**, *9*, 3084-3095.

33. Naughton, F.B.; Alibay, I.; Barnoud, J.; Barreto-Ojeda, E.; Beckstein, O.; Bouysset, C.; Cohen, O.; Gowers, R.J.; MacDermott-Opeskin, H.; Matta, M.; et al. Mdanalysis 2.0 and beyond: fast and interoperable, community driven simulation analysis. *Biophys. J* **2022**, *121*, 272-273.

34. Humphrey, W.; Dalke, A.; Schulten, K. Vmd: visual molecular dynamics. *J Mol Graph.* **1996**, *14*, 33-38.

35. Laskowski, R.A.; Swindells, M.B. Ligplot+: multiple ligand-protein interaction diagrams for drug discovery. *J Chem Inf Model.* **2011**, *51*, 2778-2786.

TOC GRAPHIC

